Reading 5: Cardiovascular measurements

Determining an individual's blood pressure is a standard clinical measurement, whether taken in a physician's office or in the hospital during a specialized surgical procedure. Blood-pressure values in the various chambers of the heart and in the peripheral vascular system help the physician determine the functional integrity of the cardiovascular system. A number of direct (invasive) and indirect (noninvasive) techniques are being used to measure blood pressure in the human. The accuracy of each should be established, as well as its suitability for a particular clinical situation.

Fluctuations in pressure recorded over the frequency range of hearing are called *sounds*. The sources of heart sounds are the vibrations set up by the accelerations and decelerations of blood.

The function of the blood circulation is to transport oxygen and other nutrients to the tissues of the body and to carry metabolic waste products away from the cells. In Section 4.6 we pointed out that the heart serves as a four-chambered pump for the circulatory system. This is illustrated in Figure 4.12. The heart is divided into two pumping systems, the right side of the heart and the left side of the heart. The pulmonary circulation and the systemic circulation separate these two pumps and their associated valves. Each pump has a filling chamber, the atrium, which helps to fill the ventricle, the stronger pump. Figure 7.15 is a diagram that shows how the electric and mechanical events are related during the cardiac cycle. The four heart sounds are also indicated in this diagram.

Figure 7.1 is a schematic diagram of the circulatory system. The left ventricle ejects blood through the aortic valve into the aorta, and the blood is then distributed through the branching network of arteries, arterioles, and capillaries. The resistance to blood flow is regulated by the arterioles, which are under local, neural, and endocrine control. The exchange of the nutrient material takes place at the capillary level. The blood then returns to the right side of the heart via the venous system. Blood fills the right atrium, the filling chamber of the right heart, and flows through the tricuspid valve into the right ventricle. The blood is pumped from the right ventricle into the pulmonary artery through the pulmonary valve. It next flows through the pulmonary arteries, arterioles, capillaries, and veins to the left atrium. At the pulmonary capillaries, O_2 diffuses from the lung alveoli to the blood,

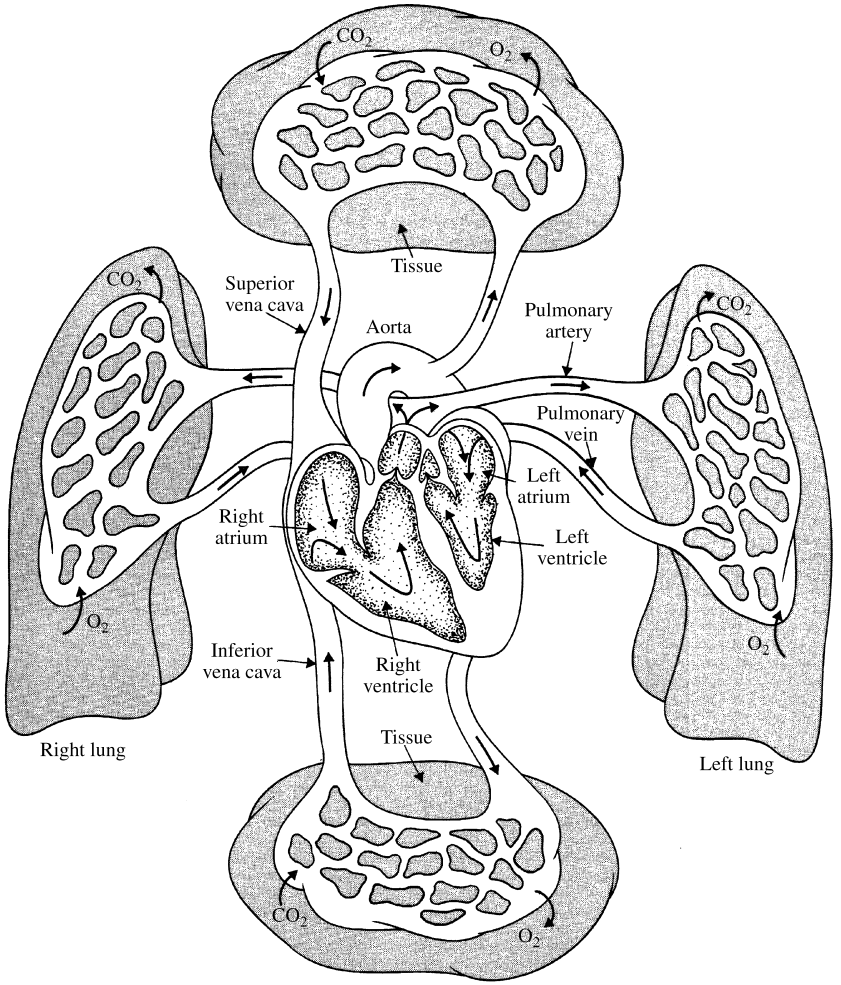

Figure 7.1 The left ventricle ejects blood into the systemic circulatory system. The right ventricle ejects blood into the pulmonary circulatory system.

and CO_2 diffuses from the blood to the alveoli. The blood flows from the left atrium, the filling chamber of the left heart, through the mitral valve into the left ventricle. When the left ventricle contracts in response to the electric stimulation of the myocardium (discussed in detail in Section 4.6), blood is pumped through the aortic valve into the aorta.

The pressures generated by the right and left sides of the heart differ somewhat in shape and in amplitude (see Figure 7.2). As we noted in Section 4.6, cardiac contraction is caused by electric stimulation of the cardiac muscle. An electric impulse is generated by specialized cells located in the sino-atrial node of the right atrium. This electric impulse quickly spreads over both atria.

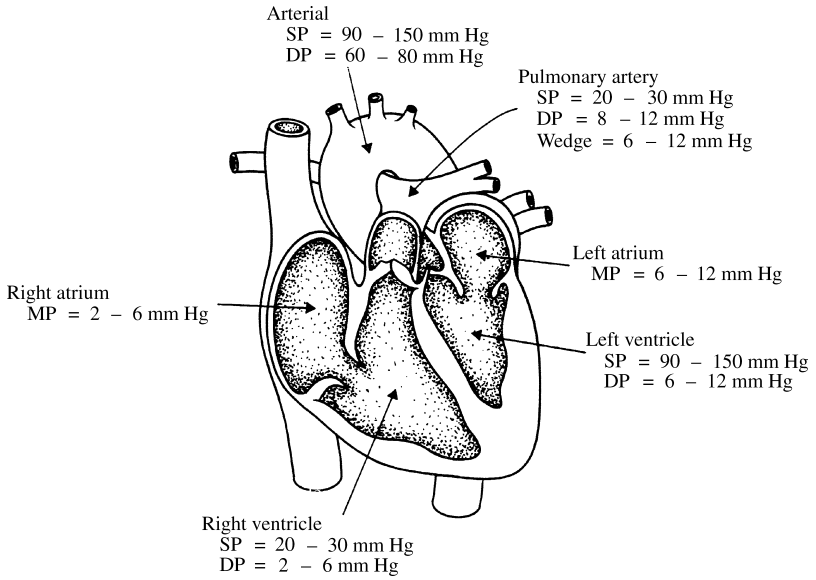

Figure 7.2 Typical values of circulatory pressures SP is the systolic pressure, DP is the diastolic pressure, and MP is the mean pressure. The wedge pressure is defined in Section 7.13.

At the junction of the atria and ventricles, the electric impulse is conducted after a short delay at the atrioventricular node. Conduction quickly spreads over the interior of both ventricles by means of a specialized conduction system, the His bundle, and the Purkinje system. Conduction then propagates throughout both ventricles. This impulse causes mechanical contraction of both ventricles. Mechanical contraction of the ventricular muscle generates ventricular pressures that force blood through the pulmonary and aortic valves into the pulmonary circulation and the systemic circulation, causing pressures in each. Section 7.9 describes the correlation of the four heart sounds with the electric and mechanical events of the cardiac cycle. Briefly, the heart sounds are associated with the movement of blood during the cardiac cycle. Murmurs are vibrations caused by the turbulence in the blood moving rapidly through the heart.

10.6 NONINVASIVE BLOOD-GAS MONITORING

Blood-gas determination can provide valuable information about the efficiency of pulmonary gas exchange, the adequacy of alveolar ventilation, blood-gas transport, and tissue oxygenation. Although invasive techniques to determine arterial blood gases are still widely practiced in many clinical situations, it is becoming apparent that simple, real-time, continuous, and noninvasive techniques offer many advantages. Most important, intermittent blood sampling provides historical data valid only at the time the sample was drawn. Delays between when the blood sample is drawn and when the blood-gas values are reported average about 30 min. Furthermore, invasive techniques are painful and have associated risks.

These limitations are particularly serious in critically ill patients for whom close monitoring of arterial blood gases is essential. Continuous noninvasive monitoring of blood gases, on the other hand, makes it possible to recognize changes in tissue oxygenation immediately and to take corrective action before irreversible cell damage occurs.

Various noninvasive techniques for monitoring arterial O_2 and CO_2 have been developed. This section describes the basic sensor principles, instrumentation, and clinical applications of the noninvasive monitoring of arterial oxygen saturation (S_{O_2}), oxygen tension (P_{O_2}), and carbon dioxide tension (P_{CO_2}).

SKIN CHARACTERISTICS

In order to appreciate the challenges of noninvasive measurement of the blood chemistry, it is important to understand the structure of the human skin. The human skin has three principal layers: the stratum corneum, epidermis, and dermis (Mendelson and Peura, 1984). These layers form a cohesive structure that typically varies in thickness from 0.2 to 2 mm, depending on the position on the body. Figure 5.7 is a schematic diagram that represents a cross section of the human skin.

The stratum corneum is the nonliving, outer layer of the skin. It is composed of a supple, protective layer of dehydrated cells. The nonvascular epidermis layer is a living tissue underneath the stratum corneum. It consists of proteins, lipids, and the melanin-forming cells (melanocytes) that give skin its color. The average thickness of the epidermis is 0.1 to 0.2 mm.

Dense connective tissue, hair follicles, sweat glands, nerve endings, fat cells, and a profuse system of capillaries make up the dermis. Here vertical capillary loops approximately 200 to 400 μm in length provide nutrients for the upper layers of the skin. Blood is supplied to these capillaries by arterioles that form a flat network parallel to the surface of the skin below the dermis. Larger arteries located in the subcutaneous tissue supply these arterioles. Venous blood in the skin is drained by venules in the upper and middle dermis and by larger veins in the subcutaneous tissue.

Arteriovenous anastomoses are innervated by nerve fibers. These shunts are found largely in the dermis of the palms, ears, and face. They regulate blood flow through the skin in response to heat; blood flow through these channels can increase to nearly 30 times the basal rate. Normal gas diffusion through the skin is low, but with increased heat—at 40 °C and above—the skin becomes more permeable to gases.

TRANSCUTANEOUS ARTERIAL OXYGEN SATURATION MONITORING (PULSE OXIMETRY)

Attempts to apply the nonpulsed two-wavelengths approach that we have discussed, which was successful for intravascular oximetry applications, to the transilluminated ear or fingertip resulted in unacceptable errors due to light attenuation by tissue and blood absorption, refraction, and multiple scattering. In addition, because of differences in the properties of skin and tissue, variation from individual to individual in attenuation of light caused large calibration problems. Oximeters can be used to measure S_{O_2} noninvasively by passing light through the pinna of the ear (Merrick and Hayes, 1976). Because of the complications caused by the light-absorbing characteristics of skin pigment and other absorbers, measurements are made at eight wavelengths and are computer-processed. The ear is warmed to 41 °C to stimulate arterial blood flow.

A two-wavelength transmission noninvasive pulse oximeter was introduced (Yoshiya *et al.*, 1980). This instrument determines S_{O_2} by analyzing the time-varying, or ac, component of the light transmitted through the skin during the systolic phase of the blood flow in the tissue (Figure 10.19). This approach achieves measurement of the arterial oxygen content with only two

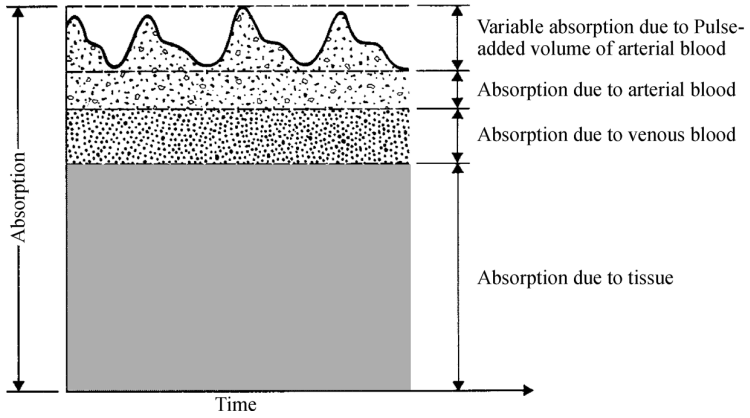

Figure 10.19 The pulse oximeter analyzes the light absorption at two wavelengths of only the pulse-added volume of oxygenated arterial blood. [From Y. M. Mendelson, "Blood gas measurement, transcutaneous,"in J. G. Webster (ed.), *Encyclopedia of Medical Devices and Instrumentation.* New York: Wiley, 1988, pp. 448–459. Used by permission.]

wavelengths (660 and 940 nm, for instance). The dc component of the transmitted light, which represents light absorption by the skin pigments and other tissues, is used to normalize the ac signals.

A transcutaneous reflectance oximeter based on a similar photoplethysmographic technique has been developed (Mendelson *et al.*, 1983). The advantage of the reflectance oximeter is that it can monitor S_{O_2} transcutaneously at various locations on the body surface, including more central locations (such as the chest, forehead, and limbs) that are not accessible via conventional transmission oximetry.

Because of these and other significant improvements in the instruments, measurements of ear, toe, and fingertip oximetry are widely used. Noninvasive measurements of S_{O_2} can be made with 2.5% accuracy for saturation values from 50% to 100%.

Transcutaneous S_{O_2} Sensor The basic transcutaneous S_{O_2} sensor, for both the transmission and the reflective mode, makes use of a light source and a photodiode. In the transmission mode, the two face each other and a segment of the body is interposed; in the reflection mode, the light source and photodiode are mounted adjacent to each other on the surface of the body (Webster, 1997).

Figure 10.20 shows an example of a transcutaneous transmission S_{O_2} sensor and monitor. These transmission sensors are placed on the fingertips, toes, ear lobes, or nose. A pair of red and infrared light-emitting diodes are used for the light source, with peak emission wavelengths of 660 nm (red) and 940 nm (infrared). These detected signals are processed, in the form of transmission photoplethysmograms, by the oximeter, which determines the S_{O_2}.

Applications of S_{O_2} Monitoring As we have noted, the applications of noninvasive S_{O_2} monitoring have blossomed rapidly to the point where it has become the standard of clinical care in a number of areas. Direct assessment and trending of the adequacy of tissue oxygenation can be made by determining the S_{O_2} value. Oximetry is applied during the administration of anesthesia, pulmonary function tests, bronchoscopy, intensive care, and oral surgery and in neonatal monitoring, sleep apnea studies, and aviation medicine.

Noninvasive oximetry is also used in the home for monitoring self-administered oxygen therapy. Noninvasive oximetry provides time-averaged blood oxygenation values and can be used to determine when immediate therapeutic intervention is necessary. A lightweight (less than 3 g) and small (20 mm diameter) optical sensor makes this transcutaneous reflectance sensor appropriate for monitoring newborns, ambulatory patients, and patients in whom a digit or earlobe is not accessible. Problems with both transmission and reflectance oximetry include poor signal with shock, interference from lights in the environment and from the presence of carboxyhemoglobin, and poor trending of transients (Payne and Severinghaus, 1986, Moyle, 1994).

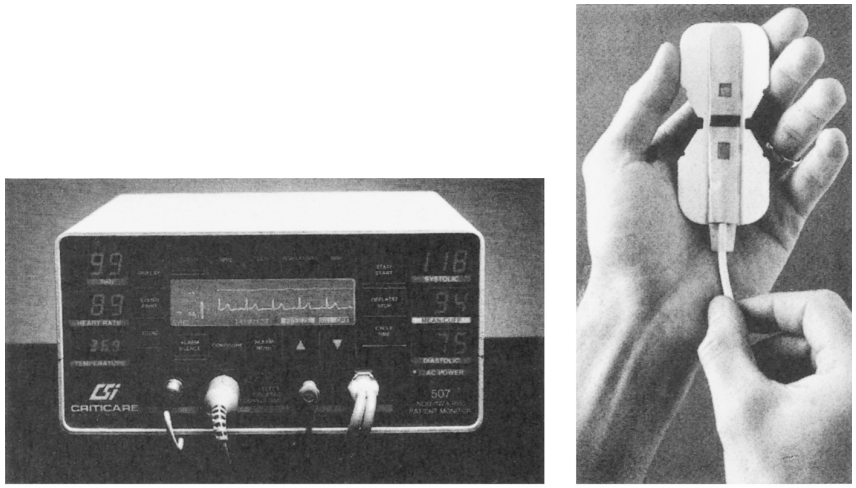

(a) (b)

Figure 10.20 (a) Noninvasive patient monitor capable of measuring ECG, noninvasive blood pressure (using automatic oscillometry), respiration (using impedance pneumography), transmission pulse oximetry, and temperature. (From Criticare Systems, Inc. Used by permission.) (b) Disposable transmission S_{O_2} sensor in open position. Note the light sources and detector, which can be placed on each side of the finger. (From Datascope Corporation. Used by permission.)

TRANSCUTANEOUS ARTERIAL OXYGEN TENSION (tcP_{O_2}) Monitoring

Measurement of tcP_{O_2} is similar in principle to the conventional in vitro P_{O_2} determination we have described. A Clark electrode is used in a sensor unit that is placed in contact with the skin. The oxygen electrode principle of operation has already been discussed.

Only two known gas mixtures are required to calibrate the sensor, because the relationship between O_2-dependent current and P_{O_2} is linear. Two calibration procedures are commonly used. One employs two precision medical gas mixtures, such as nitrogen and oxygen. The other employs sodium sulfite, which is a ''zero-O_2 solution,'' and ambient air. Good stability of the sensor is usually maintained; a drift of 1 to 2 mm Hg/h for the tcP_{O_2} sensor is typical.

Transcutaneous P_{O_2} Sensor Figure 10.21 shows a cross-sectional view of a typical Clark-type tcP_{O_2} sensor in which three glass-sealed Pt cathodes are separately connected via current amplifiers to an Ag/AgCl anode ring (Huch and Huch, 1976). A buffered KC1 electrolyte, which has a low water content to reduce drying of the sensor during storage, is used to provide a medium in which the chemical reactions can occur. Under normal physiological

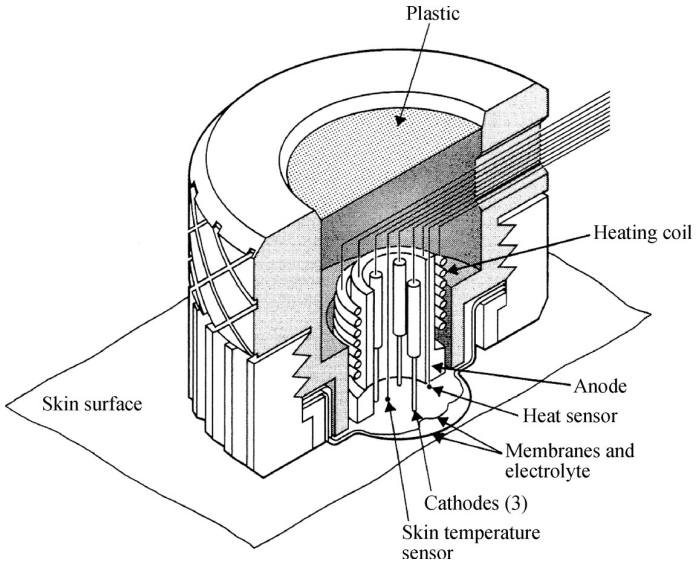

Figure 10.21 Cross-sectional view of a transcutaneous oxygen sensor. Heating promotes arterialization. (From A. Huch and R. Huch, ''Transcutaneous, noninvasive monitoring of P_{O_2},''*Hospital Practice*, 1976, 6, 43–52. Used by permission.)

conditions, the P_{O_2} at the skin surface is essentially atmospheric regardless of the P_{O_2} in the underlying tissue.

Hyperemia of the skin causes the skin P_{O_2} to approach the arterial P_{O_2}. Hyperemia can be induced by the administration of certain drugs, by the heating or abrasion of the skin, or by the application of nicotinic acid cream. Because heating gives the most readily controllable and consistent effect, a heating element and a thermistor sensor are used to control the skin temperature beneath the tcP_{O_2} sensor. Sufficient arterialization results when the skin is heated to temperatures between 43 °C and 44 °C. These temperatures cause minimal skin damage, but with neonates it is still necessary to reposition the sensor frequently to avoid burns.

Heating the skin has two beneficial effects: O_2 diffusion through the stratum corneum increases, and vasodilation of the dermal capillaries increases blood flow to skin at the sensor site where the heat is applied. Increased blood flow delivers more O_2 to the heated skin region, making the excess O_2 diffuse through the skin more easily. As Figure 10.1 suggests, heating the blood also causes the ODC to shift to the right, resulting in a decreased binding of Hb with O_2. Accordingly, the amount of O_2 released to the cells for a given P_{O_2} is increased. Note that heat also increases local tissue O_2 consumption, which tends to decrease oxygen levels in the skin tissue. Opportunely, these two opposing factors approximately cancel each other. Duration of monitoring is a function of the skin's sensitivity to possible burns, as well as to electrode drift.

Typically, continuous monitoring is recommended for 2 to 6 h before moving to a different skin site.

Applications of tcP_{O_2} Monitoring Monitoring the tcP_{O_2} has found many applications in both clinical medicine and physiological research in situations where tissue oxygenation values are important. Although tcP_{O_2} measurements are used routinely for neonates because of their thin skin, clinical results with adults have proved less valuable. The prime application of tcP_{O_2} is for newborn infants, especially those in respiratory distress (Cassady, 1983). The main reason for this application is that the need often arises to administer O_2 to sick infants, while at the same time avoiding high arterial P_{O_2}, which, in preterm infants, can lead to serious damage to retinal and pulmonary tissues. Under the opposite condition of low P_{O_2}, fetal circulation paths may be reestablished in the neonate (Huch *et al.*, 1981). Even so, because of its simpler operation, lower cost, absence of calibration, and increased reliability, noninvasive pulse oximetry has supplanted the use of tcP_{O_2} measurements in the neonate.

Good correlations between tcP_{O_2} and arterial P_{O_2} are possible when the patient is not in shock or in hypothermia. With patients who are hemodynamically compromised, tcP_{O_2} does not always equal arterial P_{O_2}. Skin heating in situations where there are significant decreases in skin blood perfusion cannot compensate for the low blood flow and the attendant low delivery of oxygen to the tissue. The result is low transcutaneous P_{O_2} readings. Examples of conditions in which skin perfusion is compromised—and tcP_{O_2} readings therefore do not represent tissue P_{O_2} values—include severe hypothermia, acidemia, anemia, and shock. Adult tcP_{O_2} values have not been found to equal arterial P_{O_2}, even when the skin is heated to 45 °C. This is due to the greater skin thickness of the adult; heating of the skin to intolerably high temperatures would be necessary to compensate for the increased metabolism. Studies have, however, demonstrated the clinical usefulness of this technique for evaluating the adequacy of cutaneous circulation in patients with peripheral resuscitation (Huch *et al.*, 1981).

Maintaining the seal between the tcP_{O_2} probe and the skin surface can be a problem with long-term monitoring. If the seal is compromised, the sensor is exposed to the atmosphere and will yield a P_{O_2} of approximately 155 mm Hg, instead of lower physiological values.

TRANSCUTANEOUS CARBON DIOXIDE TENSION (tcP_{CO_2}) MONITORING

Monitoring tcP_{CO_2} gives more accurate results than tcP_{O_2} measurements in adult patients, because tcP_{CO_2} measurements are much less dependent on skin blood flow.

Transcutaneous P_{CO_2} Sensor Figure 10.22 shows a typical tcP_{CO_2} sensor, which is similar to a tcP_{O_2} sensor except for the sensing element. Its operation

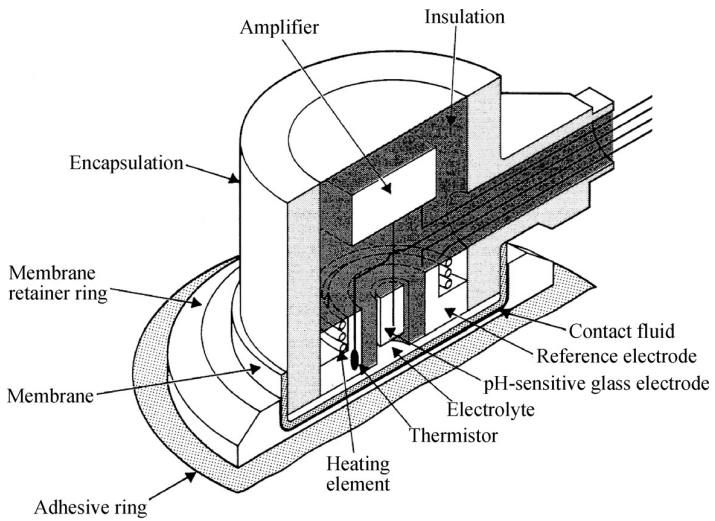

Figure 10.22 Cross-sectional view of a transcutaneous carbon dioxide sensor. Heating the skin promotes arterialization. (From A. Huch, D. W. Lübbers, and R. Huch, ''Patientenuberwachung durch transcutane P_{CO_2} Messung bei gleiechzeiliger koutrolle der relatiuen Iokalen perfusion,'' *Anaesthetist*, 1973, 22, 379. Used by permission.)

is similar to that of the electrochemical P_{CO_2} sensor described earlier. The CO_2 sensor is a glass pH electrode with a concentric Ag/AgCl reference electrode that is used as a heating element. The electrolyte, a bicarbonate buffer, is placed on the electrode surface. A CO_2-permeable Teflon membrane separates the sensor from its environment.

As we noted before, the tcP_{CO_2} sensor operates according to the Stow–Severinghaus principle; that is, a pH electrode senses a change in the CO_2 concentration. The system is calibrated with a known CO_2 concentration solution. Because a CO_2 electrode has a negative temperature coefficient, calibration must be performed at the temperature at which the device will be used. The effects of heating the skin beneath the tcP_{CO_2} sensor must be determined before the measurements can be properly interpreted.

Heating the skin beneath the sensor causes an increase in (1) P_{CO_2}, because the solubility of CO_2 decreases with an increase in temperature; (2) local tissue metabolism, because cell metabolism is directly correlated with temperature; and (3) the rate of CO_2 diffusion through the stratum corneum, which increases with temperature. As a consequence of these three effects, which all work in the same direction to increase tcP_{CO_2} values, heating the skin yields tcP_{CO_2} values larger than the corresponding arterial P_{CO_2}. Nevertheless, the correlation between tcP_{CO_2} and arterial P_{CO_2} is usually satisfactory. Because the slope of the CO_2 electrode calibration line is essentially that of the Nernst equation, a two-point calibration (as for the P_{O_2} electrode) is not needed.

Transcutaneous P_{CO_2} sensors have longer time constants than tcP_{O_2} sensors. The response time of a tcP_{CO_2} electrode varies inversely with temperature (Herrell *et al.*, 1980). *In vitro* tests have shown that the 90% response time is less than 60 s for a sensor at 44 °C. Measurements of the tcP_{CO_2} sensor response time, with step increases in the inspired CO_2, give longer time constants (Tremper *et al.*, 1981). Increasing CO_2 concentrations from 0% to 7% at different sensor and skin temperatures resulted in the time constants 15, 7.5, 5, and 3.5 min for electrode temperatures of 37 °C, 39 °C, 41 °C, and 44 °C, respectively. Note, however, that the measured response time included the response times due to CO_2 diffusion in the alveoli, capillary blood, skin, and sensor. These pronounced temperature effects can be attributed to significant changes in the structure of the stratum corneum caused by temperatures greater than 40 °C. Heating the electrode has little effect in neonates, because the stratum corneum is not fully developed.

Applications of tcPco₂ Monitoring The tcP_{CO_2} is higher than blood P_{CO_2} because epidermal cell CO_2 diffuses to the dermal capillaries in response to a diffusion gradient. A countercurrent-exchange mechanism in the dermal capillaries causes CO_2 diffusion between the parallel arterial and venous sides of the capillary bed. Arterial blood entering the rising segment of the capillary loop picks up CO_2 from the exiting venous side. As a consequence, the venous P_{CO_2} is lowered, and a maximal P_{CO_2} gradient is established at the top of the countercurrent capillary loops. Because of this phenomenon, P_{CO_2} at the skin surface is higher than venous P_{CO_2}, even when the electrode is not heated (Tremper *et al.*, 1981).

Generally, it is accepted that tcP_{CO_2} is a valuable trend monitor in neonates and adults who are not in shock. Since arterial P_{CO_2} varies linearly with alveolar ventilation, tcP_{CO_2} provides information concerning the effectiveness of spontaneous or mechanical ventilation for individuals. The extent of impaired tissue perfusion, i.e. circulation to a limb, or response to therapy may be monitored by observing the change in tcP_{CO_2}.

10.7 BLOOD-GLUCOSE SENSORS

Accurate measurement of blood glucose is essential in the diagnosis and long-term management of diabetes. This section reviews the use of biosensors for continuous measurement of glucose levels in blood and other body fluids.

Glucose is the main circulating carbohydrate in the body. In normal, fasting individuals, the concentration of glucose in blood is very tightly regulated—usually between 80 and 90 mg/100 ml, during the first hour or so following a meal. The hormone insulin, which is normally produced by beta cells in the pancreas, promotes glucose transport into skeletal muscle and adipose tissue. In those suffering from diabetes mellitus, insulin-regulated uptake is compromised, and blood glucose can reach concentrations ranging from 300 to 700 mg/100 ml (hyperglycemia).

Accurate determination of glucose levels in body fluids, such as blood, urine, and cerebrospinal fluid, is a major aid in diagnosing diabetes and improving the treatment of this disease. Blood glucose levels rise and fall several times a day, so it is difficult to maintain normoglycemia by means of an ''open-loop'' insulin delivery approach. One solution to this problem would be to ''close the loop'' by using a self-adapting insulin infusion device with a glucose-controlled biosensor that could continuously sense the need for insulin and dispense it at the correct rate and time. Unfortunately, present-day glucose sensors cannot meet this stringent requirement (Peura and Mendelson, 1984).

Glucose Oxidase Method The glucose oxidase method used in a large number of commercially available simple test strip meters allows quick and easy blood glucose measurements. A test strip product, One Touch UltraMini (www.LifeScan.com), depends on the glucose oxidase–peroxidase chromogenic reaction. After a drop of blood is combined with reagents on the test strip, the reaction shown in (10.18) occurs.

$$\text{Glucose} + 2H_2O + O_2 \xrightarrow{\text{glucose oxidase}} \text{Gluconic Acid} + 2H_2O_2 \qquad (10.18)$$

Adding the enzymes peroxidase and o-dianiside, a chromogenic oxygen, results in the formation of a colored compound that can be evaluated visually.

$$\text{o-dianisine} + H_2O_2 \xrightarrow{\text{peroxidase}} \text{oxidized o-dianisine} + H_2O \qquad (10.19)$$

Glucose oxidase chemistry in conjunction with reflectance photometry produces a system for monitoring blood glucose levels (Burtis and Ashwood, 1994). In the One Touch system (Figure 10.23), a test strip is inserted into the meter, a drop of blood is applied to end of the test strip, and a digital screen displays the results 5 s later.

Electroenzymatic Approach Electroenzymatic sensors based on polarographic principles utilize the phenomenon of glucose oxidation with a glucose oxidase enzyme (Clark and Lyons, 1962). The chemical reaction of glucose with oxygen is catalyzed in the presence of glucose oxidase. This causes a decrease in the partial pressure of oxygen (P_{O_2}), an increase in pH, and the production of hydrogen peroxide by the oxidation of glucose to gluconic acid according to equation (10.18).

Investigators measure changes in all of these chemical components in order to determine the concentration of glucose. The basic glucose enzyme electrode utilizes a glucose oxidase enzyme immobilized on a membrane or a gel matrix, and an oxygen-sensitive polarographic electrode. Changes in oxygen concentration at the electrode, which are due to the catalytic reaction of glucose and oxygen, can be measured either amperometrically or potentiometrically.

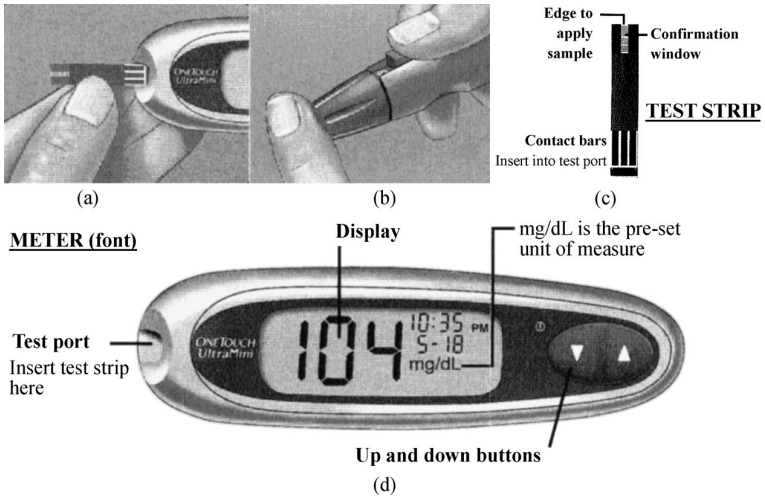

Figure 10.23 (a) A test strip is inserted into the meter. (b) A lance is released to lance the skin less than 1 mm. (c) The 1 μL blood sample is applied to the end of the test strip and drawn into it by capillary action. (d) Then 5 s later, the meter displays the blood glucose in mg/dL.

Because a single-electrode technique is sensitive both to glucose and to the amount of oxygen present in the solution, a modification to remove the oxygen response by using two polarographic oxygen electrodes has been suggested (Updike and Hicks, 1967). Figure 10.24 illustrates both the principle of the enzyme electrode and the dual-cathode enzyme electrode. An active enzyme is placed over the glucose electrode, which senses glucose and oxygen. The other electrode senses only oxygen. The amount of glucose is determined as a function of the difference between the readings of these two electrodes. More recently, development of hydrophobic membranes that are more permeable to oxygen than to glucose has been described (Gilligan *et al.*, 2004). Placing these membranes over a glucose enzyme electrode solves the problem associated with oxygen limitation and increases the linear response of the sensor to glucose.

The major problem with enzymatic glucose sensors is the instability of the immobilized enzyme and the fouling of the membrane surface under physiological conditions. Most glucose sensors operate effectively only for short periods of time. In order to improve the present sensor technologies, more highly selective membranes must be developed. The features that must be taken into account in designing and fabricating these membranes include the diffusion rate of both oxygen and glucose from the external medium to the surface of the membrane, diffusion and concentration gradients within the membrane, immobilization of the enzyme, and the stability of the enzymatic reaction (Jaffari and Turner, 1995).

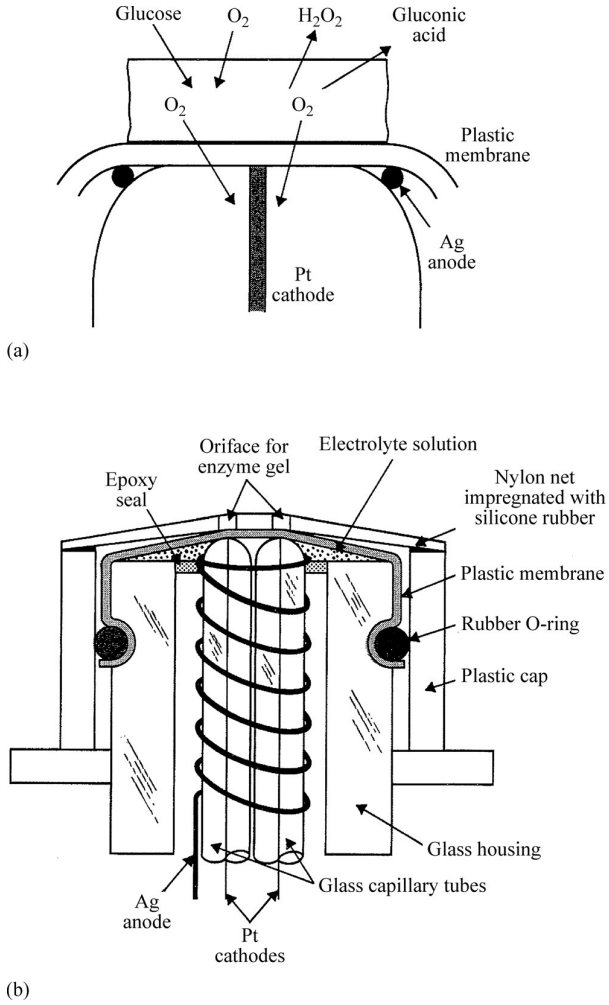

Figure 10.24 (a) In the enzyme electrode, when glucose is present it combines with O_2, so less O_2 arrives at the cathode. (b) In the dual-cathode enzyme electrode, one electrode senses only O_2 and the difference signal measures glucose independent of O_2 fluctuations. (From S. J. Updike and G. P. Hicks, "The enzyme electrode, a miniature chemical transducer using immobilized enzyme activity,"*Nature*, 1967, 214, 986–988. Used by permission.)

Optical Approach A number of innovative glucose sensors, based on different optical techniques, has been developed in recent years. A new fluorescence-based affinity sensor has been designed for monitoring various metabolites, especially glucose in the blood plasma (Schultz *et al.*, 1982). The method is similar in principle to that used in radioimmunoassays. It is based

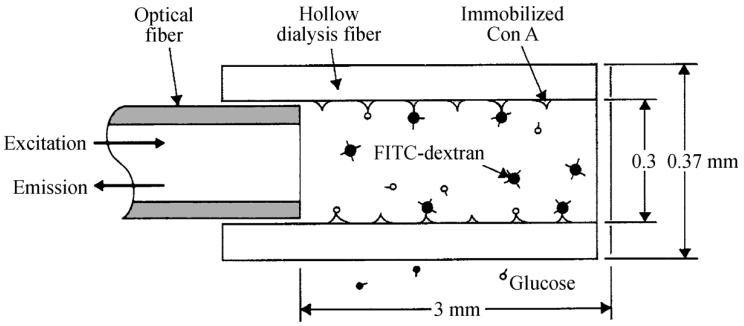

Figure 10.25 The affinity sensor measures glucose concentration by detecting changes in fluorescent light intensity caused by competitive binding of a fluorescein-labeled indicator. (From J. S. Schultz, S. Manouri, *et al.*, ''Affinity sensor: A new technique for developing implantable sensors for glucose and other metabolites,''*Diabetes Care*, 1982 5, 245–253. Used by permission.)

on the immobilized competitive binding of a particular metabolite and fluorescein-labeled indicator with receptor sites specific for the measured metabolite and the labeled ligand (the molecule that binds).

Figure 10.25 shows an affinity sensor in which the immobilized reagent is coated on the inner wall of a glucose-permeable hollow fiber fastened to the end of an optical fiber. The fiber-optic catheter is used to detect changes in fluorescent light intensity, which is related to the concentration of glucose. These researches have demonstrated the simplicity of the sensor and the feasibility of its miniaturization, which could lead to an implantable glucose sensor. Figure 10.26 is a schematic diagram of the optical system for the affinity sensor. The advantage of this approach is that it has the potential for miniaturization and for implantation through a needle. In addition, as with other fiber-optic approaches, no electric connections to the body are necessary.

The major problems with this approach are the lack of long-term stability of the reagent, the slow response time of the sensor, and the dependence of the measured light intensity on the amount of reagent, which is usually very small and may change over time.

EXTRAVASCULAR SENSORS

The extravascular sensor system is made up of a catheter connected to a three-way stopcock and then to the pressure sensor (Figure 7.3). The catheter–sensor system, which is filled with a saline–heparin solution, must be flushed with the solution every few minutes to prevent blood from clotting at the tip.

The physician inserts the catheter either by means of a surgical cut-down, which exposes the artery or vein, or by means of percutaneous insertion, which

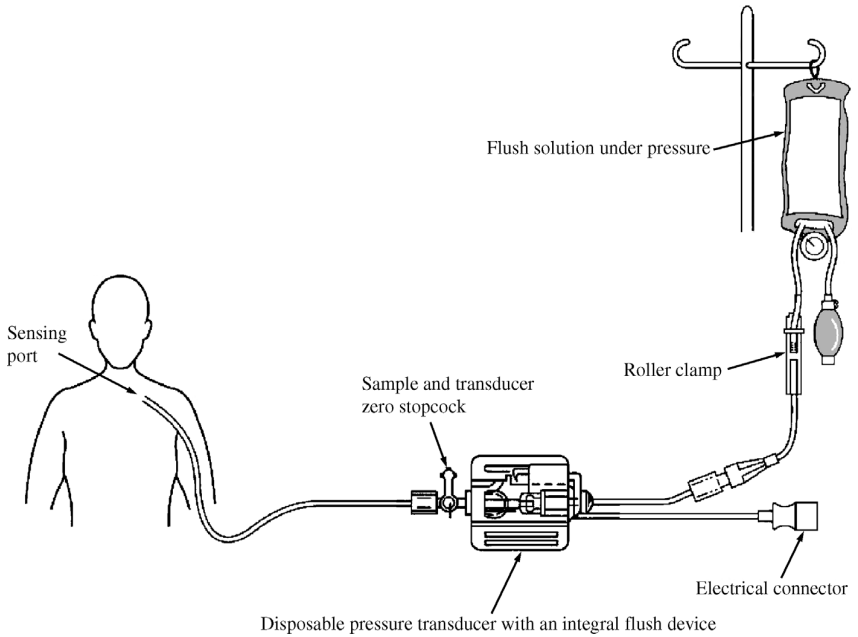

Figure 7.3 Extravascular pressure-sensor system A catheter couples a flush solution (heparinized saline) through a disposable pressure sensor with an integral flush device to the sensing port. The three-way stopcock is used to take blood samples and zero the pressure sensor.

involves the use of a special needle or guide-wire technique. Blood pressure is transmitted via the catheter liquid column to the sensor and, finally, to the diaphragm, which is deflected. Figure 2.2(a) shows an early pressure sensor, in which the displacement of the diaphragm is transmitted to a system composed of a moving armature and an unbonded strain gage. Figure 2.5 shows a modern disposable blood-pressure sensor.

INTRAVASCULAR SENSORS

Catheter-tip sensors have the advantage that the hydraulic connection via the catheter, between the source of pressure and the sensor element, is eliminated. The frequency response of the catheter–sensor system is limited by the hydraulic properties of the system. Detection of pressures at the tip of the catheter without the use of a liquid-coupling system can thus enable the physician to obtain a high frequency response and eliminate the time delay encountered when the pressure pulse is transmitted in a catheter–sensor system.

A number of basic types of sensors are being used commercially for the detection of pressure in the catheter tip. These include various types of strain-gage systems bonded onto a flexible diaphragm at the catheter tip. Gages of this type are available in the F 5 catheter [1.67 mm outer diameter (OD)] size. In the French scale (F), used to denote the diameter of catheters, each unit is approximately equal to 0.33 mm. Smaller-sized catheters may become available as the technology improves and the problems of temperature and electric drift, fragility, and nondestructive sterilization are solved more satisfactorily. A disadvantage of the catheter-tip pressure sensor is that it is more expensive than others and may break after only a few uses, further increasing its cost per use.

The fiber-optic intravascular pressure sensor can be made in sizes comparable to those described above, but at a lower cost. The fiber-optic device measures the displacement of the diaphragm optically by the varying reflection of light from the back of the deflecting diaphragm. (Recall that Section 2.14 detailed the principles of transmission of light along a fiber bundle.) These devices are inherently safer electrically, but unfortunately they lack a convenient way to measure relative pressure without an additional lumen either connected to a second pressure sensor or vented to the atmosphere.

A fiber-optic microtip sensor for *in vivo* measurements inside the human body is shown in Figure 7.4 (a) in which one leg of a bifurcated fiber bundle is connected to a light-emitting diode (LED) source and the other to a photodetector (Hansen, 1983). The pressure-sensor tip consists of a thin metal membrane mounted at the common end of the mixed fiber bundle. External pressure causes membrane deflection, varying the coupling between the LED source and the photodetector. Figure 7.4(b) shows the output signal versus membrane deflection. Optical fibers have the property of emitting and accepting light within a cone defined by the acceptance angle θ_A, which is equal to the fiber numerical aperture, N_A (Section 2.14). The coupling between LED source and detector is a function of the overlap of the two acceptance angles

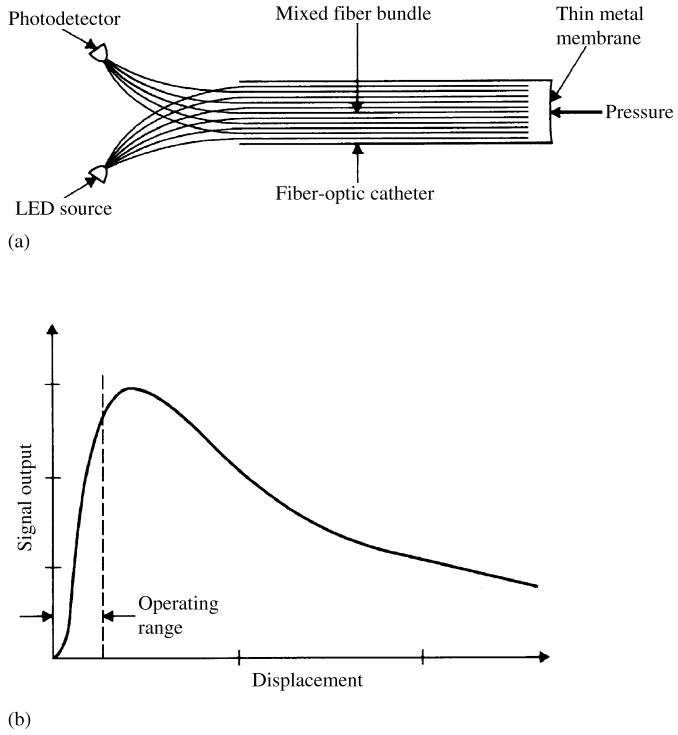

Figure 7.4 (a) Schematic diagram of an intravascular fiber-optic pressure sensor. Pressure causes deflection in a thin metal membrane that modulates the coupling between the source and detector fibers. (b) Characteristic curve for the fiber-optic pressure sensor.

on the pressure-sensor membrane. The operating portion of the curve is the left slope region where the characteristic is steepest.

7.9 HEART SOUNDS

The auscultation of the heart gives the clinician valuable information about the functional integrity of the heart. More information becomes available when clinicians compare the temporal relationships between the heart sounds and the mechanical and electric events of the cardiac cycle. This latter approach is known as *phonocardiography*.

There is a wide diversity of opinion concerning the theories that attempt to explain the origin of heart sounds and murmurs. More than 40 different mechanisms have been proposed to explain the first heart sound. A basic definition shows the difference between heart sounds and murmurs (Rushmer, 1970). Heart sounds are vibrations or sounds due to the acceleration or deceleration of blood, whereas murmurs are vibrations or sounds due to blood turbulence.

MECHANISM AND ORIGIN

Figure 7.15 shows how the four heart sounds are related to the electric and mechanical events of the cardiac cycle. The first heart sound is associated with the movement of blood during ventricular systole (Rushmer, 1970). As the ventricles contract, blood shifts toward the atria, closing the atrioventricular valves with a consequential oscillation of blood. The first heart sound further originates from oscillations of blood between the descending root of the aorta and ventricle and from vibrations due to blood turbulence at the aortic and pulmonary valves. Splitting of the first heart sound is defined as an asynchronous closure of the tricuspid and mitral valves. The second heart sound is a low-frequency vibration associated with the deceleration and reversal of flow in the aorta and pulmonary artery and with the closure of the semilunar valves (the valves situated between the ventricles and the aorta or the pulmonary trunk).

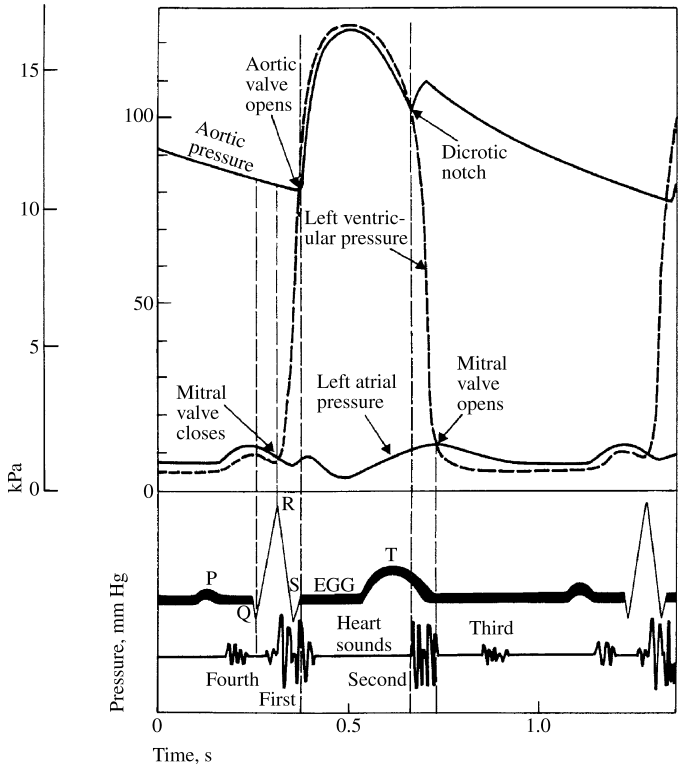

Figure 7.15 Correlation of the four heart sounds with electric and mechanical events of the cardiac cycle.

This second heart sound is coincident with the completion of the T wave of the ECG.

The third heart sound is attributed to the sudden termination of the rapid-filling phase of the ventricles from the atria and the associated vibration of the ventricular muscle walls, which are relaxed. This low-amplitude, low-frequency vibration is audible in children and in some adults.

The fourth or atrial heart sound—which is not audible but can be recorded by the phonocardiogram—occurs when the atria contract and propel blood into the ventricles.

The sources of most murmurs, developed by turbulence in rapidly moving blood, are known. Murmurs during the early systolic phase are common in children, and they are normally heard in nearly all adults after exercise. Abnormal murmurs may be caused by stenoses and insufficiencies (leaks) at the aortic, pulmonary, and mitral valves. They are detected by noting the time of their occurrence in the cardiac cycle and their location at the time of measurement.

AUSCULTATION TECHNIQUES

Heart sounds travel through the body from the heart and major blood vessels to the body surface. Because of the acoustical properties of the transmission path, sound waves are attenuated and not reflected. The largest attenuation of the wavelike motion occurs in the most compressible tissues, such as the lungs and fat layers.

There are optimal recording sites for the various heart sounds, sites at which the intensity of sound is the highest because the sound is being transmitted through solid tissues or through a minimal thickness of inflated lung. There are four basic chest locations at which the intensity of sound from the four valves is maximized (Figure 7.16).

Heart sounds and murmurs have extremely small amplitudes, with frequencies from 0.1 to 2000 Hz. Two difficulties may result. At the low end of the spectrum (below about 20 Hz), the amplitude of heart sounds is below the threshold of audibility. The high-frequency end is normally quite perceptible to the human ear, because this is the region of maximal sensitivity. However, if a phonocardiogram is desired, the recording device must be carefully selected for high frequency-response characteristics. That is, a light-beam, ink-jet, or digital-array recorder would be adequate, whereas a standard pen strip-chart recorder would not.

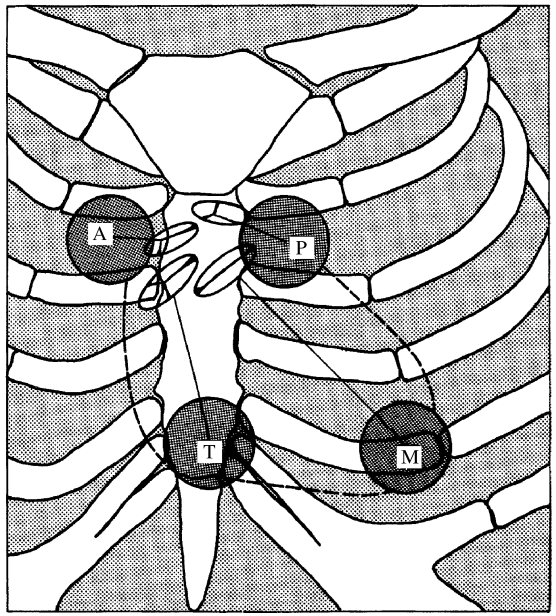

Figure 7.16 **Auscultatory areas on the chest** A, aortic; P, pulmonary; T, tricuspid; and M, mitral areas. (From A. C. Burton, *Physiology and Biophysics of the Circulation*, 2nd ed. Copyright © 1972 by Year Book Medical Publishers, Inc., Chicago. Used by permission.)

Because heart sounds and murmurs are of low amplitude, extraneous noises must be minimized in the vicinity of the patient. It is standard procedure to record the phonocardiogram for nonbedridden patients in a specially designed, acoustically quiet room. Artifacts from movements of the patient appear as baseline wandering.

STETHOSCOPES

Stethoscopes are used to transmit heart sounds from the chest wall to the human ear. Some variability in interpretation of the sounds stems from the user's auditory acuity and training. Moreover, the technique used to apply the stethoscope can greatly affect the sounds perceived.

Ertel *et al.* (1966a; 1966b) have investigated the acoustics of stethoscope transmission and the acoustical interactions of human ears with stethoscopes. They found that stethoscope acoustics reflected the acoustics of the human ear. Younger individuals revealed slightly better responses to a stethoscope than their elders. The mechanical stethoscope amplifies sound because of a standing-wave phenomenon that occurs at quarter wavelengths of the sound. Figure 7.17 is a typical frequency-response curve for a stethoscope; it shows that the mechanical stethoscope has an uneven frequency response, with many resonance peaks.

These investigators emphasized that the critical area of the performance of a stethoscope (the clinically significant sounds near the listener's threshold of hearing) may be totally lost if the stethoscope attenuates them as little 3 dB.

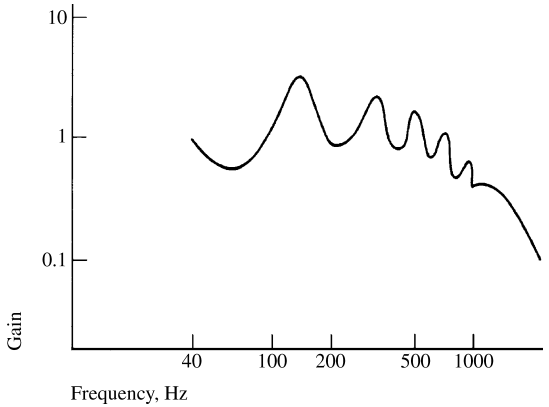

Figure 7.17 The typical frequency-response curve for a stethoscope can be found by applying a known audio-frequency signal to the bell of a stethoscope by means of a headphone-coupler arrangement. The audio output of the stethoscope earpiece was monitored by means of a coupler microphone system. (From Ertel *et al.* (1966); by permission of American Heart Association.)

A physician may miss, with one instrument, sounds that can be heard with another.

When the stethoscope chest piece is firmly applied, low frequencies are attenuated more than high frequencies. The stethoscope housing is in the shape of a bell. It makes contact with the skin, which serves as the diaphragm at the bell rim. The diaphragm becomes taut with pressure, thereby causing an attenuation of low frequencies.

Loose-fitting earpieces cause additional problems, because the leak that develops reduces the coupling between the chest wall and the ear, with a consequent decrease in the listener's perception of heart sounds and murmurs.

Stethoscopes are also useful for listening to the sounds caused by airflow obstruction or lung collapse (Loudon and Murphy, 2006).

Engineers have proposed many types of electronic stethoscopes. These devices have selectable frequency-response characteristics ranging from the ''ideal'' flat-response case and selected bandpasses to typical mechanical-stethoscope responses. Physicians, however, have not generally accepted these electronic stethoscopes, mainly because they are unfamiliar with the sounds heard with them. Their size, portability, convenience, and resemblance to the mechanical stethoscope are other important considerations.

7.13 INDIRECT MEASUREMENTS OF BLOOD PRESSURE

Indirect measurement of blood pressure is an attempt to measure intra-arterial pressures noninvasively. The most standard manual techniques employ either the palpation or the auditory detection of the pulse distal to an occlusive cuff. Figure 7.20 shows a typical system for indirect measurement of blood pressure. It employs a sphygmomanometer consisting of an inflatable cuff for occlusion of the blood vessel, a rubber bulb for inflation of the cuff, and either a mercury or an aneroid manometer for detection of pressure.

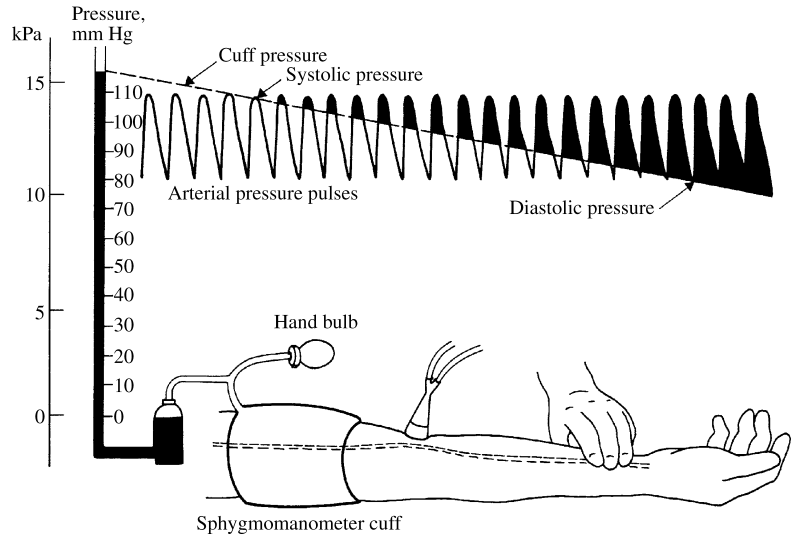

Figure 7.20 Typical indirect blood-pressure measurement system The sphygmomanometer cuff is inflated by a hand bulb to pressure above the systolic level. Pressure is then slowly released, and blood flow under the cuff is monitored by a microphone or stethoscope placed over a downstream artery. The first Korotkoff sound detected indicated systolic pressure, whereas the transition from muffling to silence brackets diastolic pressure. (From R.F. Rushmer, *Cardiovascular Dynamics*, 3rd ed., 1970. Philadelphia: W.B. Saunders Co. Used with permission.)

Blood pressure is measured in the following way. The occlusive cuff is inflated until the pressure is above systolic pressure and then is slowly bled off (2 to 3 mm Hg/s) (0.3 to 0.4 kPa/s). When the systolic peaks are higher than the occlusive pressure, the blood spurts under the cuff and causes a palpable pulse in the wrist (Riva–Rocci method). Audible sounds (Korotkoff sounds) generated by the flow of blood and vibrations of the vessel under the cuff are heard through a stethoscope. The manometer pressure at the first detection of the pulse indicates the systolic pressure. As the pressure in the cuff is decreased, the audible Korotkoff sounds pass through five phases (Geddes, 1970). The period of transition from muffling (phase IV) to silence (phase V) brackets the diastolic pressure.

In employing the palpation and auscultatory techniques, you should take several measurements, because normal respiration and vasomotor waves modulate the normal blood-pressure levels. These techniques also suffer from the disadvantage of failing to give accurate pressures for infants and hypotensive patients.

Using an occlusive cuff of the correct size is important if the clinician is to obtain accurate results. The pressure applied to the artery wall is assumed to be equal to that of the external cuff. However, the cuff pressure is transmitted via interposed tissue. With a cuff of sufficient width and length, the cuff pressure is evenly transmitted to the underlying artery. It is generally accepted that the width of the cuff should be about 0.40 times the circumference of the extremity. However, no general agreement appears to exist about the length of the pneumatic cuff (Geddes, 1970). If a short cuff is used, it is important that it be positioned over the artery of interest. A longer cuff reduces the problem of misalignment. The cuff should be placed at heart level to avoid hydrostatic effects.

The auscultatory technique is simple and requires a minimum of equipment. However, it cannot be used in a noisy environment, whereas the palpation technique can. The hearing acuity of the user must be good for low frequencies from 20 to 300 Hz, the bandwidth required for these measurements. Bellville and Weaver (1969) have determined the energy distribution of the Korotkoff sounds for normal patients and for patients in shock. When there is a fall in blood pressure, the sound spectrum shifts to lower frequencies. The failure of the auscultation technique for hypotensive patients may be due to low sensitivity of the human ear to these low-frequency vibrations (Geddes, 1970).

There is a common misconception that normal human blood pressure is 120/80, meaning that the systolic value is 120 mm Hg (16 kPa) and that the diastolic value is 80 mm Hg (10.7 kPa). This is not the case. A careful study (by Master *et al*., 1952) showed that the age and sex of an individual determine the ''normal value'' of blood pressure.

A number of techniques have been proposed to measure automatically and indirectly the systolic and diastolic blood pressure in humans (Cobbold, 1974). The basic technique involves an automatic sphygmomanometer that inflates and deflates an occlusive cuff at a predetermined rate. A sensitive detector is used to measure the distal pulse or cuff pressure. A number of kinds of detectors have been employed, including ultrasonic, piezoelectric, photoelectric, electroacoustic, thermometric, electrocardiographic, rheographic, and tissue-impedance devices (Greatorex, 1971; Visser and Muntinga, 1990). Three of the commonly used automatic techniques are described in the following paragraphs.

The first technique employs an automated auscultatory device wherein a microphone replaces the stethoscope. The cycle of events that takes place begins with a rapid (20 to 30 mm Hg/s) (2.7 to 4 kPa/s) inflation of the occlusive cuff to a preset pressure about 30 mm Hg higher than the suspected systolic level. The flow of blood beneath the cuff is stopped by the collapse of the vessel. Cuff pressure is then reduced slowly (2 to 3 mm Hg/s) (0.3 to 0.4 kPa/s). The first Korotkoff sound is detected by the microphone, at which time the level of the cuff pressure is stored. The muffling and silent period of the Korotkoff sounds is detected, and the value of the diastolic pressure is also stored. After a few minutes, the instrument displays the systolic and diastolic pressures and recycles the operation. Design considerations for various types of automatic indirect methods of measurement of blood pressure can be found in the literature (Greatorex, 1971).

The ultrasonic determination of blood pressure employs a transcutaneous Doppler sensor that detects the motion of the blood-vessel walls in various states of occlusion. Figure 7.21 shows the placement of the compression cuff over two small transmitting and receiving ultrasound crystals (8 MHz) on the arm (Stegall *et al*., 1968). The Doppler ultrasonic transmitted signal is focused on the vessel wall and the blood. The reflected signal (shifted in frequency) is detected by the receiving crystal and decoded (Section 8.4). The difference in frequency, in the range of 40 to 500 Hz, between the transmitted and received signals is proportional to the velocity of the wall motion and the blood velocity. As the cuff pressure is increased above diastolic but below systolic, the vessel opens and closes with each heartbeat, because the pressure in the artery oscillates above and below the applied external pressure in the cuff. The opening and closing of the vessel are detected by the ultrasonic system.

As the applied pressure is further increased, the time between the opening and closing decreases until they coincide. The reading at this point is the systolic pressure. Conversely, when the pressure in the cuff is reduced, the time between opening and closing increases until the closing signal from one pulse coincides with the opening signal from the next. The reading at this point is the diastolic pressure, which prevails when the vessel is open for the complete pulse.

The advantages of the ultrasonic technique are that it can be used with infants and hypotensive individuals and in high-noise environments. A disadvantage is that movements of the subject's body cause changes in the ultrasonic path between the sensor and the blood vessel. Complete reconstruction of the arterial-pulse waveform is also possible via the ultrasonic method. A timing pulse from the ECG signal is used as a reference. The clinician uses the pressure in the cuff when the artery opens versus the time

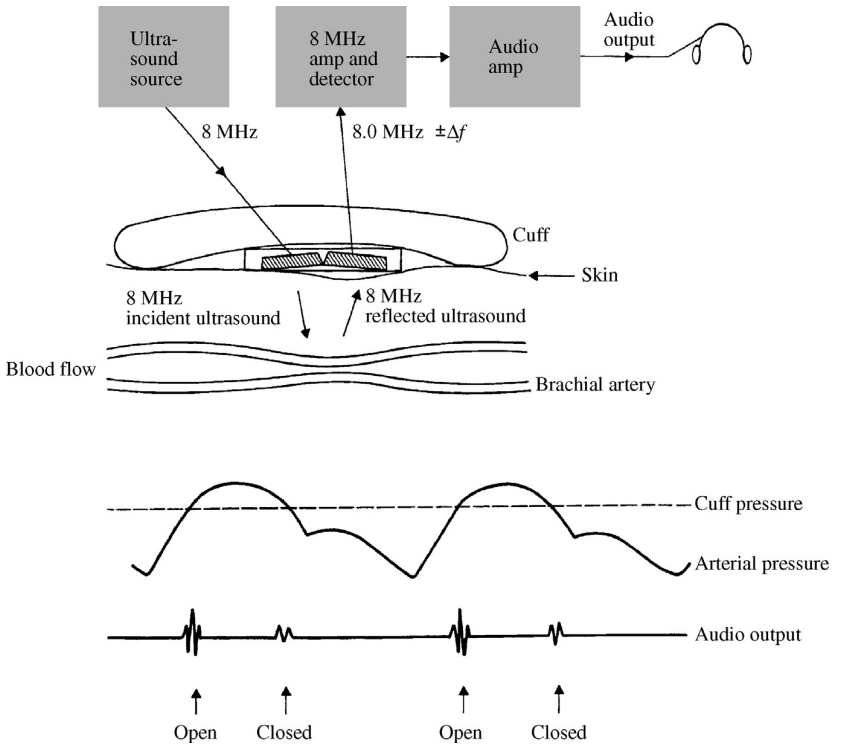

Figure 7.21 Ultrasonic determination of blood pressure A compression cuff is placed over the transmitting (8 MHz) and receiving ($8\,\text{MHz} \pm \Delta f$) crystals. The opening and closing of the blood vessel are detected as the applied cuff pressure is varied. (From H. F. Stegall, M. B. Kardon, and W. T. Kemmerer, ''Indirect measurement of arterial blood pressure by Doppler ultrasonic sphygmomanometry.'' *J. Appl. Physiol.*, 1968, 25, 793–798. Used with permission.)

from the ECG R wave to plot the rising portion of the arterial pulse. Conversely, the clinician uses the cuff pressure when the artery closes versus the time from the ECG R wave to plot the falling portion of the arterial pulse.

The oscillometric method, a noninvasive blood pressure technique, measures the amplitude of oscillations that appear in the cuff pressure signal which are created by expansion of the arterial wall each time blood is forced through the artery. The uniqueness of the oscillometric method, a blood-pressure cuff technique, is that specific characteristics of the compression cuff's entrained air volume are used to identify and sense blood-pressure values. The cuff-pressure signal increases in strength in the systolic pressure region, reaching a maximum when the cuff pressure is equal to mean arterial pressure. As the cuff pressure drops below this point, the signal strength decreases proportionally to the cuff air pressure bled rate. There is no clear transition in cuff-pressure oscillations to identify diastolic pressure since arterial wall expansion continues to happen below diastolic pressure while blood is forced through the artery (Geddes, 1984). Thus, oscillometric monitors employ proprietary algorithms to estimate the diastolic pressure.

Ramsey (1991) has indicated that, using the oscillometric method, the mean arterial pressure is the single blood-pressure parameter, which is the most robust measurement, as compared with systolic and diastolic pressure, because it is measured when the oscillations of cuff pressure reach the greatest amplitude. This property usually allows mean arterial pressure to be measured reliably even in case of hypotension with vasoconstriction and diminished pulse pressure.

When the cuff pressure is raised quickly to pressures higher than systolic pressure it is observed that the radial pulse disappears. Cuff pressures above systolic cause the underlying artery to be completely occluded. However, at suprasystolic cuff pressures, small amplitude pressure oscillations occur in the cuff pressure due to artery pulsations under the upper edge of the cuff, which are communicated to the cuff through the adjacent tissues. With slow cuff-pressure reductions, when the cuff pressure is just below systolic pressure, blood spurts through the artery and the cuff-pressure oscillations become larger. Figure 7.22 illustrates the ideal case in which the cuff pressure is monitored by a pressure sensor connected to a strip chart recorder. A pressure slightly above systolic pressure is detected by determining the shift from small-amplitude oscillations at cuff pressure slightly above systolic pressure and when the cuff pressure begins to increase amplitude (point 1). As the cuff

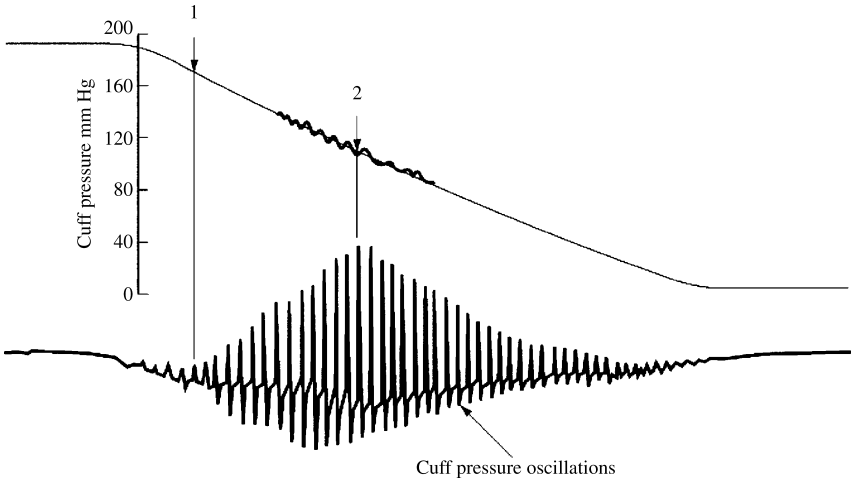

Figure 7.22 The oscillometric method A compression cuff is inflated above systolic pressure and slowly deflated. Systolic pressure is detected (point 1) where there is a transition from small amplitude oscillations (above systolic pressure) to increasing cuff-pressure amplitude. The cuff-pressure oscillations increase to a maximum (point 2) at the mean arterial pressure.

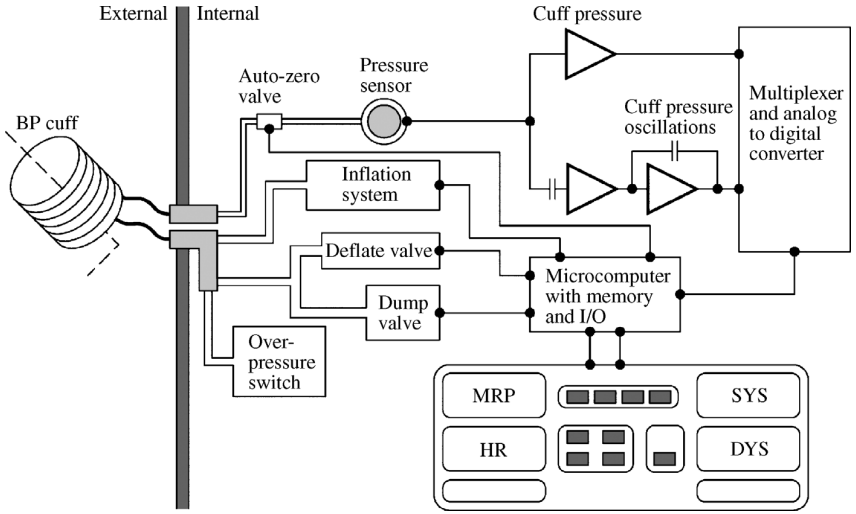

Figure 7.23 Block diagram of the major components and subsystems of an oscillometric blood-pressure monitoring device, based on the Dinamap unit, I/O = input/output; MAP = mean arterial pressure; HR = heart rate; SYS = systolic pressure; DYS = diastolic pressure. [From Ramsey M III. Blood Pressure monitoring: automated oscillometric devices, *J. Clin. Monit.* 1991, 7, 56–67]

continues to deflate, the amplitude of the oscillations increases reaching a maximum, and then decreases as the cuff pressure is decreased to zero. Point 2 in Figure 7.22 is the maximum cuff-pressure oscillation, which is essentially true mean arterial pressure. Since there is no apparent transition in the oscillation amplitude as cuff pressure passes diastolic pressure, algorithmic methods are used to predict diastolic pressure.

The system description begins with the blood-pressure cuff, which compresses a limb and its vasculature by the encircling inflatable compression cuff pressures (Ramsey, 1991). The cuff is connected to a pneumatic system (see Figure 7.23). A solid-state pressure sensor senses cuff pressure, and the electric signal proportional to pressure is processed in two different circuits. One circuit amplifies and corrects the zero offset of the cuff-pressure signal before the analog-to-digital digitization. The other circuit high-pass filters and amplifies the cuff-pressure signal. Cuff pressure is controlled by a microcomputer that activates the cuff inflation and deflation systems during the measurement cycle.

Blood flow

One of the primary measurements the physician would like to acquire from a patient is that of the concentration of O_2 and other nutrients in the cells. Such quantities are normally so difficult to measure that the doctor is forced to accept the second-class measurements of blood flow and changes in blood volume, which usually correlate with concentration of nutrients. If blood *flow* is difficult to measure, the physician may settle for the third-class measurement of blood *pressure*, which usually correlates adequately with blood flow. If blood pressure cannot be measured, the physician may fall back on the fourth-class measurement of the ECG, which usually correlates adequately with blood pressure.

Note that the measurement of blood flow—the main subject of this chapter—is the one that most closely reflects the primary measurement of concentration of O_2 in the cells. However, measurement of blood flow is usually more difficult to make and more invasive than measurement of blood pressure or of the ECG.

Commonly used flowmeters, such as the orifice or turbine flowmeters, are unsuitable for measuring blood flow because they require cutting the vessel and can cause formation of clots. The specialized techniques described in this chapter have therefore been developed.

8.1 INDICATOR-DILUTION METHOD THAT USES CONTINUOUS INFUSION

The indicator-dilution methods described in this chapter do not measure instantaneous pulsatile flow but, rather, flow averaged over a number of heartbeats.

CONCENTRATION

When a given quantity m_0 of an indicator is added to a volume V, the resulting concentration C of the indicator is given by $C = m_0/V$. When an additional

quantity m of indicator is then added, the incremental increase in concentration is $\Delta C = m/V$. When the fluid volume in the measured space is continuously removed and replaced, as in a flowing stream, then in order to maintain a fixed change in concentration, the clinician must continuously add a fixed quantity of indicator per unit time. That is, $\Delta C = (dm/dt)/(dV/dt)$. From this equation, we can calculate flow (Donovan and Taylor, 2006).

$$F = \frac{dV}{dt} = \frac{dm/dt}{\Delta C} \tag{8.1}$$

EXAMPLE 8.1 Derive (8.1) using principles of mass transport.

ANSWER The rate at which indicator enters the vessel is equal to the indicator's input concentration C_i, times the flow F. The rate at which indicator is injected into the vessel is equal to the quantity per unit time, dm/dt. The rate at which indicator leaves the vessel is equal to the indicator's output concentration C_o times F. For steady state, $C_iF + dm/dt = C_oF$ or $F = (dm/dt)/(C_o - C_i)$.

FICK TECHNIQUE

We can use (8.1) to measure *cardiac output* (blood flow from the heart) as follows (Capek and Roy, 1988):

$$F = \frac{dm/dt}{C_a - C_v} \tag{8.2}$$

where

F = blood flow, liters/min
dm/dt = consumption of O_2, liters/min
C_a = arterial concentration of O_2, liters/liter
C_v = venous concentration of O_2, liters/liter

Figure 8.1 shows the measurements required. The blood returning to the heart from the upper half of the body has a different concentration of O_2 from the blood returning from the lower half, because the amount of O_2 extracted by the brain is different from that extracted by the kidneys, muscles, and so forth. Therefore, we cannot accurately measure C_v in the right atrium. We must measure it in the pulmonary artery after it has been mixed by the pumping action of the right ventricle. The physician may float the catheter into place by temporarily inflating a small balloon surrounding the tip. This is done through a second lumen in the catheter.

As the blood flows through the lung capillaries, the subject adds the indicator (the O_2) by breathing in pure O_2 from a spirometer (see Figure 9.6).

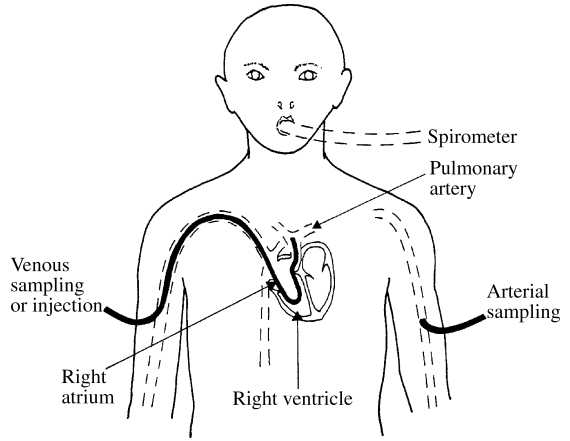

Figure 8.1 Several methods of measuring cardiac output In the Fick method, the indicator is O_2; consumption is measured by a spirometer. The arterial-venous concentration difference is measured by drawing samples through catheters placed in an artery and in the pulmonary artery. In the dye-dilution method, dye is injected into the pulmonary artery and samples are taken from an artery. In the thermodilution method, cold saline is injected into the right atrium and temperature is measured in the pulmonary artery.

The exhaled CO_2 is absorbed in a soda-lime canister, so the consumption of O_2 is indicated directly by the net gas-flow rate.

The clinician can measure the concentration of the oxygenated blood C_a in any artery, because blood from the lung capillaries is well mixed by the left ventricle and there is no consumption of O_2 in the arteries. An arm or leg artery is generally used.

EXAMPLE 8.2 Calculate the cardiac output, given the following data: spirometer O_2 consumption 250 ml/min; arterial O_2 content, 0.20 ml/ml; venous O_2 content, 0.15 ml/ml.

ANSWER From (8.2),

$$\begin{aligned} F &= \frac{dm/dt}{C_a - C_v} \\ &= \frac{0.25 \text{ liter/min}}{(0.20 \text{ liter/liter}) - (0.15 \text{ liter/liter})} \\ &= 5 \text{ liters/min} \end{aligned} \tag{8.3}$$

The units for the concentrations of O_2 represent the volume of O_2 that can be extracted from a volume of blood. This concentration is very high for blood, because large quantities of oxygen can be bound to hemoglobin. It would be

very low if water were flowing through the vessels, even if the PO_2 were identical in both cases.

The Fick technique is nontoxic, because the indicator (O_2) is a normal metabolite that is partially removed as blood passes through the systemic capillaries. The cardiac output must be constant over several minutes so that the investigator can obtain the slope of the curve for O_2 consumption. The presence of the catheter causes a negligible change in cardiac output.

8.2 INDICATOR-DILUTION METHOD THAT USES RAPID INJECTION

EQUATION

The continuous-infusion method has been largely replaced by the rapid-injection method, which is more convenient. A bolus of indicator is rapidly injected into the vessel, and the variation in downstream concentration of the indicator versus time is measured until the bolus has passed. The solid line in Figure 8.2 shows the fluctuations in concentration of the indicator that occur after the injection. The dotted-line extension of the exponential decay shows the curve that would result if there were no recirculation. For this case we can calculate the flow as outlined in the following paragraphs.

An increment of blood of volume dV passes the sampling site in time dt. The quantity of indicator dm contained in dV is the concentration $C(t)$ times the incremental volume. Hence $dm = C(t)dV$. Dividing by dt, we obtain $dm/dt = C(t)dV/dt$. But $dV/dt = F_i$, the instantaneous flow; therefore

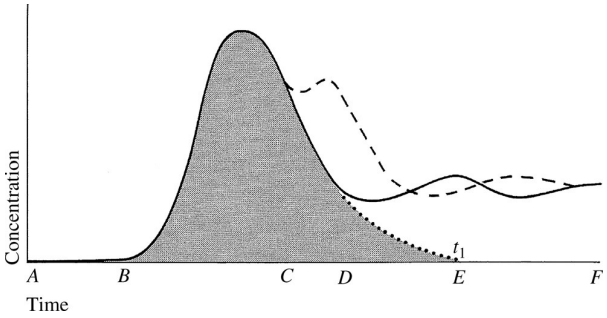

Figure 8.2 **Rapid-injection indicator-dilution curve** After the bolus is injected at time A, there is a transportation delay before the concentration begins rising at time B. After the peak is passed, the curve enters an exponential decay region between C and D, which would continue decaying along the dotted curve to t_1 if there were no recirculation. However, recirculation causes a second peak at E before the indicator becomes thoroughly mixed in the blood at F. The dashed curve indicates the rapid recirculation that occurs when there is a hole between the left and right sides of the heart.

$dm = F_i C(t)dt$. Integrating over time through t_1, when the bolus has passed the downstream sampling point, we obtain

$$m = \int_0^{t_1} F_i C(t)dt \tag{8.4}$$

where t_1 is the time at which all effects of the first pass of the bolus have died out (point E in Figure 8.2). The mixing of the bolus and the blood within the heart chambers and the lungs smooths out minor variations in the instantaneous flow F_i produced by the heartbeat. Thus we can obtain the average flow F from

$$F = \frac{m}{\int_0^{t_1} C(t)dt} \tag{8.5}$$

The integrated quantity in (8.5) is equal to the shaded area in Figure 8.2, and we can obtain it by counting squares or using a planimeter. A computer can extrapolate the dotted line in real time and compute the flow.

If the initial concentration of indicator is not zero—as may be the case when there is residual indicator left over from previous injections—then (8.5) becomes

$$F = \frac{m}{\int_0^{t_1} [\Delta C(t)]\, dt} \tag{8.6}$$

DYE DILUTION

A common method of clinically measuring cardiac output is to use a colored dye, *indocyanine green* (cardiogreen). It meets the necessary requirements for an indicator in that it is (1) inert, (2) harmless, (3) measurable, (4) economical, and (5) always intravascular. In addition, its optical absorption peak is 805 nm, the wavelength at which the optical absorption coefficient of blood is independent of oxygenation. The dye is available as a liquid that is diluted in isotonic saline and injected directly through a catheter, usually into the pulmonary artery. About 50% of the dye is excreted by the kidneys in the first 10 min, so repeat determinations are possible.

The plot of the curve for concentration versus time is obtained from a constant-flow pump, which draws blood from a catheter placed in the femoral or brachial artery. Blood is drawn through a colorimeter cuvette (Figure 2.17), which continuously measures the concentration of dye, using the principle of absorption photometry (Section 11.1). The 805 nm channel of a two-channel blood oximeter can be used for measuring dye-dilution curves. The clinician

calibrates the colorimeter by mixing known amounts of dye and blood and drawing them through the cuvette.

The shape of the curve can provide additional diagnostic information. The dashed curve in Figure 8.2 shows the result when a left-right shunt (a hole between the left and right sides of the heart) is present. Blood recirculates faster than normal, resulting in an earlier recirculation peak. When a right-left shunt is present, the delay in transport is abnormally short, because some dye reaches the sampling site without passing through the lung vessels.

THERMODILUTION

The most common method of measuring cardiac output is that of injecting a bolus of cold saline as an indicator. A special four-lumen catheter (Trautman and D'ambra, 2006) is floated through the brachial vein into place in the pulmonary artery. A syringe forces a gas through one lumen; the gas inflates a small, doughnut-shaped balloon at the tip. The force of the flowing blood carries the tip into the pulmonary artery. The cooled saline indicator is injected through the second lumen into the right atrium. The indicator is mixed with blood in the right ventricle. The resulting drop in temperature of the blood is detected by a thermistor located near the catheter tip in the pulmonary artery. The third lumen carries the thermistor wires. The fourth lumen, which is not used for the measurement of thermodilution, can be used for withdrawing blood samples. The catheter can be left in place for about 24 h, during which time many determinations of cardiac output can be made, something that would not be possible if dye were being used as the indicator. Also, it is not necessary to puncture an artery.

We can derive the following equation, which is analogous to (8.6).

$$F = \frac{Q}{\rho_b C_b \int_0^{t_1} \Delta T_b(t)\, dt} \text{ (m}^3\text{/s)} \tag{8.7}$$

where

Q = heat content of injectate, J($= V_i \Delta T_i \rho_i c_i$)
ρ_b = density of blood, kg/m^3
c_b = specific heat of blood, J/(kg·K)

When an investigator uses the thermodilution method, there are a number of problems that cause errors. (1) There may be inadequate mixing between the injection site and the sampling site. (2) There may be an exchange of heat between the blood and the walls of the heart chamber. (3) There is heat exchange through the catheter walls before, during, and after injection. However, the instrument can be calibrated by simultaneously performing dye-dilution determinations and applying a correction factor that corrects for several of the errors.

8.3 ELECTROMAGNETIC FLOWMETERS

The electromagnetic flowmeter measures instantaneous pulsatile flow of blood and thus has a greater capability than indicator-dilution methods, which measure only average flow. It operates with any conductive liquid, such as saline or blood.

PRINCIPLE

The electric generator in a car generates electricity by induction. Copper wires move through a magnetic field, cutting the lines of magnetic flux and inducing an emf in the wire. This same principle is exploited in a commonly used blood flowmeter, shown in Figure 8.3. Instead of copper wires, the flowmeter depends on the movement of blood, which has a conductance similar to that of saline. Faraday's law of induction gives the formula for the induced emf.

$$e = \int_0^{L_1} \mathbf{u} \times \mathbf{B} \cdot d\mathbf{L}$$

where

$\mathbf{B}$ = magnetic flux density, T
$\mathbf{L}$ = length between electrodes, m
$\mathbf{u}$ = instaneous velocity of blood, m/s

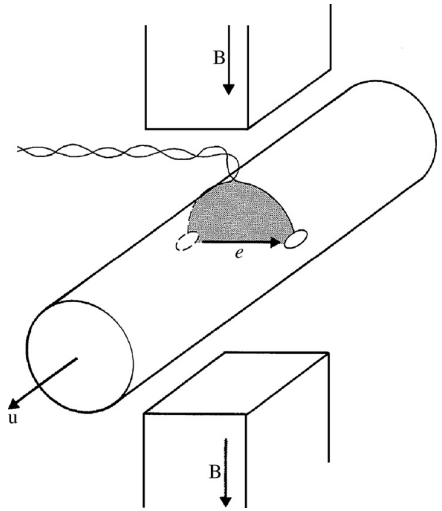

Figure 8.3 Electromagnetic flowmeter When blood flows in the vessel with velocity $\mathbf{u}$ and passes through the magnetic field $\mathbf{B}$, the induced emf e is measured at the electrodes shown. When an ac magnetic field is used, any flux lines cutting the shaded loop induce an undesired transformer voltage.

For a uniform magnetic field B and a uniform velocity profile u, the induced emf is

$$e = BLu \tag{8.8}$$

where these three components are orthogonal.

Let us now consider real flowmeters, several of which exhibit a number of divergences from this ideal case. If the vessel's cross section were square and the electrodes extended the full length of two opposite sides, the flowmeter would measure the correct average flow for any flow profile. The electrodes are small, however, so velocities near them contribute more to the signal than do velocities farther away.

Figure 8.4 shows the weighting function that characterizes this effect for circular geometry. It shows that the problem is less when the electrodes are located outside the vessel wall. The instrument measures correctly for a uniform flow profile. For axisymmetric nonuniform flow profiles, such as the parabolic flow profile resulting from laminar flow, the instrument measurement is correct if u is replaced by $\bar{u}$, the average flow velocity. Because we usually know the cross-sectional area A of the lumen of the vessel, we can multiply A by $\bar{u}$ to obtain F, the volumetric flow. However, in many locations of blood vessels in the body, such as around the curve of the aorta and near its branches, the velocity profile is asymmetric, so errors result.

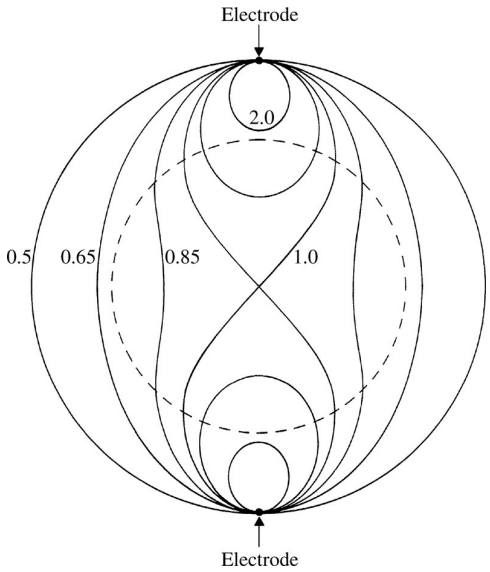

Figure 8.4 Solid lines show the weighting function that represents relative velocity contributions (indicated by numbers) to the total induced voltage for electrodes at the top and bottom of the circular cross section. If the vessel wall extends from the outside circle to the dashed line, the range of the weighting function is reduced. (Adapted from J. A. Shercliff, *The Theory of Electromagnetic Flow Measurement*, © 1962, Cambridge University Press.)

Other factors can also cause error.

1. Regions of high velocity generate higher incremental emfs than regions of low velocity, so circulating currents flow in the transverse plane. These currents cause varying drops in resistance within the conductive blood and surrounding tissues.
2. The ratio of the conductivity of the wall of the blood vessel to that of the blood varies with the *hematocrit* (percentage of cell volume to blood volume), so the shunting effects of the wall cause a variable error.
3. Fluid outside the wall of the vessel has a greater conductivity than the wall, so it shunts the flow signal.
4. The magnetic-flux density is not uniform in the transverse plane; this accentuates the problem of circulating current.
5. The magnetic-flux density is not uniform along the axis, which causes circulating currents to flow in the axial direction.

To minimize these errors, most workers recommend calibration for animal work by using blood from the animal—and, where possible, the animal's own vessels also. Blood or saline is usually collected in a graduated cylinder and timed with a stopwatch.

8.4 ULTRASONIC FLOWMETERS

The ultrasonic flowmeter, like the electromagnetic flowmeter, can measure instantaneous flow of blood. The ultrasound can be beamed through the skin, thus making transcutaneous flowmeters practical. Advanced types of ultrasonic flowmeters can also measure flow profiles. These advantages are making the ultrasonic flowmeter the subject of intensive development. Let us examine some aspects of this development.

TRANSDUCERS

For the transducer to be used in an ultrasonic flowmeter, we select a piezoelectric material (Section 2.6) that converts power from electric to acoustic form (Christensen, 1988). Lead zirconate titanate is a crystal that has the highest conversion efficiency. It can be molded into any shape by melting. As it is cooled through the Curie temperature, it is placed in a strong electric field to polarize the material. It is usually formed into disks that are coated on opposite faces with metal electrodes and driven by an electronic oscillator. The resulting electric field in the crystal causes mechanical constriction. The pistonlike movements generate longitudinal plane waves, which propagate into the tissue. For maximal efficiency, the crystal is one-half wavelength thick. Any cavities between the crystal and the tissue must be filled with a fluid or watery gel in order to prevent the high reflective losses associated with liquid–gas interfaces.

Because the transducer has a finite diameter, it will produce diffraction patterns, just as an aperture does in optics. Figure 8.8 shows the outline of the beam patterns for several transducer diameters and frequencies. In the *near field*, the beam is largely contained within a cylindrical outline and there is little spreading. The intensity is not uniform, however: There are multiple maximums and minimums within this region, caused by interference. The near field extends a distance d_{nf} given by

$$d_{nf} = \frac{D^2}{4\lambda} \tag{8.9}$$

where D = transducer diameter and λ = wavelength.

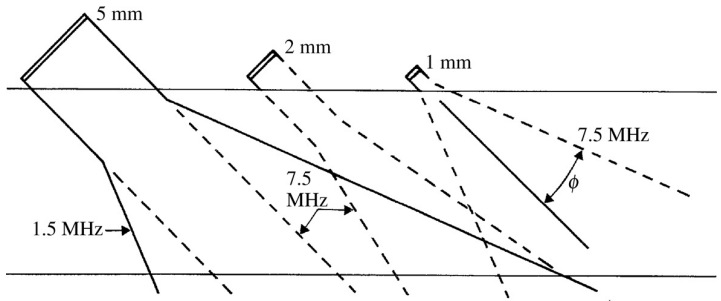

Figure 8.8 Near and far fields for various transducer diameters and frequencies. Beams are drawn to scale, passing through a 10 mm-diameter vessel. Transducer diameters are 5, 2, and 1 mm. Solid lines are for 1.5 MHz, dashed lines for 7.5 MHz.

In the *far field* the beam diverges, and the intensity is inversely proportional to the square of the distance from the transducer. The angle of beam divergence ϕ, shown in Figure 8.8, is given by

$$\sin\phi = \frac{1.2\lambda}{D} \tag{8.10}$$

Figure 8.8 indicates that we should avoid the far field because of its lower spatial resolution. To achieve near-field operation, we must use higher frequencies and larger transducers.

To select the operating frequency, we must consider several factors. For a beam of constant cross section, the power decays exponentially because of absorption of heat in the tissue. The absorption coefficient is approximately proportional to frequency, so this suggests a low operating frequency. However, most ultrasonic flowmeters depend on the power scattered back from moving red blood cells. The backscattered power is proportional to f^4, which suggests a high operating frequency. The usual compromise dictates a frequency between 2 and 10 MHz.

TRANSIT-TIME FLOWMETER

Figure 8.9(a) shows the transducer arrangement used in the transit-time ultrasonic flowmeter (Christensen, 1988). The effective velocity of sound in the vessel is equal to the velocity of sound, c, plus a component due to $\hat{u}$, the velocity of flow of blood averaged along the path of the ultrasound. For laminar flow, $\hat{u} = 1.33\,\overline{u}$, and for turbulent flow, $\hat{u} = 1.07\,\overline{u}$, where $\overline{u}$ is the velocity of the flow of blood averaged over the cross-sectional area. Because the ultrasonic path is along a single line rather than averaged over the cross-sectional area, $\hat{u}$ differs from $\overline{u}$. The transit time in the downstream (+) and upstream (−) directions is

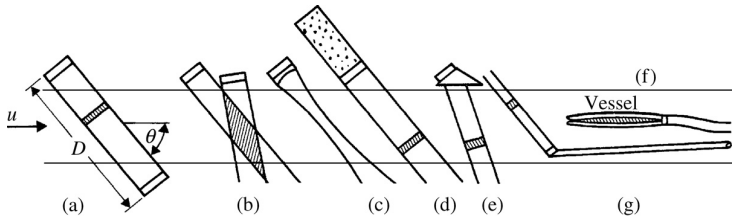

Figure 8.9 Ultrasonic transducer configurations (a) A transit-time probe requires two transducers facing each other along a path of length D inclined from the vessel axis at an angle ϕ. The hatched region represents a single acoustic pulse traveling between the two transducers. (b) In a transcutaneous probe, both transducers are placed on the same side of the vessel, so the probe can be placed on the skin. Beam intersection is shown hatched. (c) Any transducer may contain a plastic lens that focuses and narrows the beam. (d) For pulsed operation, the transducer is loaded by backing it with a mixture of tungsten powder in epoxy. This increases losses and lowers Q. Shaded region is shown for a single time of range gating. (e) A shaped piece of Lucite on the front loads the transducer and also refracts the beam. (f) A transducer placed on the end of a catheter beams ultrasound down the vessel. (g) For pulsed operation, the transducer is placed at an angle.

$$t = \frac{\text{distance}}{\text{conduction velocity}} = \frac{D}{c \pm \hat{u}\cos\theta} \tag{8.11}$$

The difference between upstream and downstream transit times is

$$\Delta t = \frac{2\,D\hat{u}\cos\theta}{(c^2 - \hat{u}^2\cos^2\theta)} \cong \frac{2\,D\hat{u}\cos\theta}{c^2} \tag{8.12}$$

and thus the average velocity $\hat{u}$ is proportional to Δt. A short acoustic pulse is transmitted alternately in the upstream and downstream directions. Unfortunately, the resulting Δt is in the nanosecond range, and complex electronics are required to achieve adequate stability. Like the electromagnetic flowmeter, the transit-time flowmeter and similar flowmeters using a phase-shift principle can operate with either saline or blood as a fluid, because they do not require particulate matter for scattering. However, they do require invasive surgery to expose the vessel.

CONTINUOUS-WAVE DOPPLER FLOWMETER

When a target recedes from a fixed source that transmits sound, the frequency of the received sound is lowered because of the Doppler effect. For small changes, the fractional change in frequency equals the fractional change in velocity.

$$\frac{f_d}{f_0} = \frac{u}{c} \tag{8.13}$$

where

f_d = Doppler frequency shift
f_0 = source frequency
u = target velocity
c = velocity of sound

The flowmeter shown in Figure 8.10 requires particulate matter such as blood cells to form reflecting targets. The frequency is lowered twice. One shift occurs between the transmitting source and the moving cell that receives the

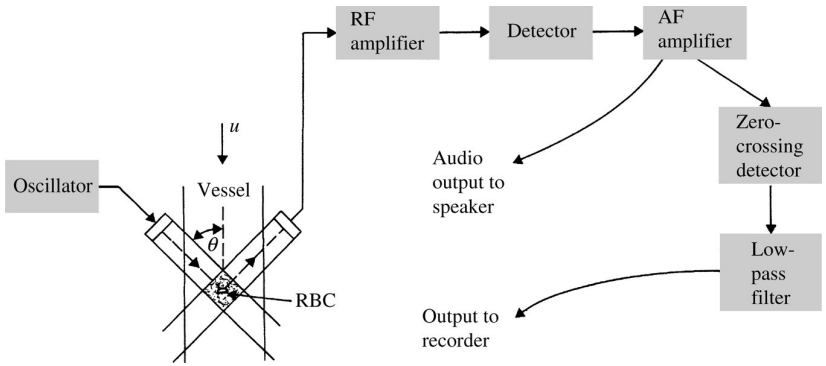

Figure 8.10 Doppler ultrasonic blood flowmeter In the simplest instrument, ultrasound is beamed through the vessel walls, backscattered by the red blood cells, and received by a piezoelectric crystal.

signal. The other shift occurs between the transmitting cell and the receiving transducer.

$$\frac{f_d}{f_0} = \frac{2u}{c+u} \cong \frac{2u}{c} \tag{8.14}$$

The approximation is valid, because $c \cong 1500$ m/s and $u \cong 1.5$ m/s. The velocities do not all act along the same straight line, so we add an angle factor

$$f_d = \frac{2 f_0 u \cos\theta}{c} \tag{8.15}$$

where θ is the angle between the beam of sound and the axis of the blood vessel, as shown in Figure 8.10. If the flow is not axial, or the transducers do not lie at the same angle, such as in Figure 8.9(b), we must include additional trigonometric factors.

Figure 8.10 shows the block diagram of a simple continuous-wave flowmeter. The oscillator must have a low output impedance to drive the low-impedance crystal. Although at most frequencies the crystal transducer has a high impedance, it is operated at mechanical resonance, where the impedance drops to about 100 Ω. The ultrasonic waves are transmitted to the moving cells, which reflect the Doppler-shifted waves to the receiving transducer. The receiving transducer is identical to the transmitting transducer. The amplified radio-frequency (RF) signal plus carrier signal is detected to produce an audio-frequency (AF) signal at a frequency given by (8.15).

Listening to the audio output using a speaker, we get much useful qualitative information. A simple *frequency-to-voltage converter* provides a quantitative output to a recorder. The *zero-crossing detector* emits a fixed-area pulse each time the audio signal crosses the zero axis. These pulses are low-pass-filtered to produce an output proportional to the velocity of the blood cells.

Although the electromagnetic blood flowmeter is capable of measuring both forward and reverse flow, the simple ultrasonic-type flowmeter full-wave rectifies the output, and the sense of direction of flow is lost. This results because—for either an increase or a decrease in the Doppler-shifted frequency—the beat frequency is the same. Examination of the field intersections shown in Figure 8.10 suggests that the only received frequency is the Doppler-shifted one. However, the received carrier signal is very much larger than the desired Doppler-shifted signal. Some of the RF carrier is coupled to the receiver by the electric field from the transmitter. Because of side lobes in the transducer apertures, some of the carrier signal travels a direct acoustic path to the receiver. Other power at the carrier frequency reaches the receiver after one or more reflections from fixed interfaces. The resulting received signal is composed of a large-amplitude signal at the carrier frequency plus the very low (approximately 0.1%) amplitude Doppler-shifted signal.

The Doppler-shifted signal is not at a single frequency, as implied by (8.15), for several reasons.

1. Velocity profiles are rarely blunt, with all cells moving at the same velocity. Rather, cells move at different velocities, producing different shifts of the Doppler frequency.
2. A given cell remains within the beam-intersection volume for a short time. Thus the signal received from one cell is a pure frequency multiplied by some time-gate function, yielding a band of frequencies.
3. Acoustic energy traveling within the main beam, but at angles to the beam axis, plus energy in the side lobes, causes different Doppler-frequency shifts due to an effective change in θ.
4. Tumbling of cells and local velocities resulting from turbulence cause different Doppler-frequency shifts.

All these factors combine to produce a band of frequencies. The resulting spectrum is similar to band-limited random noise, and from this we must extract flow information.

We would like to have high gain in the RF amplifier in order to boost the low-amplitude Doppler-frequency components. But the carrier is large, so the gain cannot be too high or saturation will occur. The RF bandwidth need not be wide, because the frequency deviation is only about 0.001 of the carrier frequency. However, RF-amplifier bandwidths are sometimes much wider than required, to permit tuning to different transducers.

The detector can be a simple square-law device such as a diode. The output spectrum contains the desired difference (beat) frequencies, which lie in the audio range, plus other undesired frequencies.

EXAMPLE 8.4 Calculate the maximal audio frequency of a Doppler ultrasonic blood flowmeter that has a carrier frequency of 7 MHz, a transducer angle of 45°, a blood velocity of 150 cm/s, and an acoustic velocity of 1500 m/s.

ANSWER Substitute these data into (8.15).

$$f_d = \frac{2(7 \times 10^6 \text{ Hz})(1.5 \text{ m/s}) \cos 45^\circ}{1500 \text{ m/s}} \cong 10 \text{ kHz} \tag{8.16}$$

8.8 PHOTOPLETHYSMOGRAPHY

Light can be transmitted through a capillary bed. As arterial pulsations fill the capillary bed, the changes in volume of the vessels modify the absorption, reflection, and scattering of the light. Although photoplethysmography is simple and indicates the timing of events such as heart rate, it provides a poor measure of changes in volume, and it is very sensitive to motion artifact.

LIGHT SOURCES

Figure 8.20 shows two photoplethysmographic methods, in which sources generate light that is transmitted through the tissue (Geddes and Baker, 1989). A miniature tungsten lamp may be used as the light source, but the

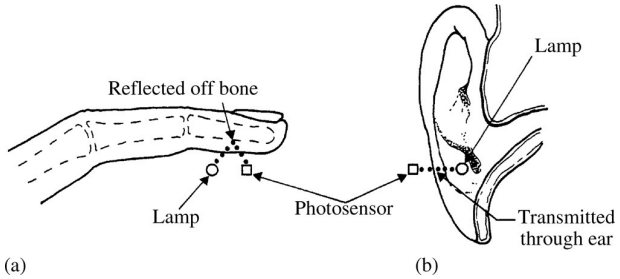

Figure 8.20 (a) Light transmitted into the finger pad is reflected off bone and detected by a photosensor. (b) Light transmitted through the aural pinna is detected by a photosensor.

heat generated causes vasodilation, which alters the system being measured. This may be considered desirable, however, because a larger pulse is produced. A less bulky unit may be formed using a GaAs LED (Lee *et al*., 1975), which produces a narrow-band source with a peak spectral emission at a wavelength of 940 nm [Figure 2.18(a)].

PHOTOSENSORS

Photoconductive cells have been used as sensors, but they are bulky and present a problem in that prior exposure to light changes the sensitivity of the cell. In addition, a filter is required to restrict the sensitivity of the sensor to the near-infrared region so that changes in blood O_2 content that are prominent in the visible-light region will not cause changes in sensitivity. A less bulky unit can be formed using an Si phototransistor. A filter that passes only infrared light is helpful for all types of sensors to prevent 120 Hz signals from fluorescent lights from being detected. This does not prevent dc light from tungsten lights or daylight from causing baseline shifts, so lightproof enclosures are usually provided for these devices.

CIRCUITS

The output from the sensor represents a large value of transmittance, modulated by very small changes due to pulsations of blood. To eliminate the large baseline value, frequencies above 0.05 Hz are passed through a high-pass filter. The resulting signal is greatly amplified to yield a sufficiently large waveform. Any movement of the photoplethysmograph relative to the tissue causes a change in the baseline transmittance that is many times larger than the pulsation signal. These large artifacts due to motion saturate the amplifier; thus it is a good thing to have a means of quickly restoring the output trace.

Gas flow measurement

Pneumotachometers The flow sensors that historically have been, and continue to be, the mainstay of the respiratory laboratory utilize flow resistors with approximately linear pressure–flow relationships. These devices are usually referred to as *pneumotachometers* (Macia, 2006). (In general, the term *pneumotachometer* is synonymous with *gas volume flowmeter.)* Flow-resistance pneumotachometers are easy to use and can distinguish the directions of alternating flows. They also have sufficient accuracy, sensitivity, linearity, and frequency response for most clinical applications. In addition, they use the same differential pressure sensors and amplifiers required for other respiratory measurements. The following discussion primarily concerns these instruments.

Even though other flow-resistance elements have been incorporated in pneumotachometers, those most commonly used consist of either one (Silverman and Whittenberger, 1950) or more (Sullivan *et al.,* 1984) fine mesh screens [Figure 9.3(a)] placed perpendicular to flow, or a tightly packed bundle of capillary tubes or channels [Figure 9.3(b)] with its axis parallel to flow (Fleisch, 1925). These physical devices exhibit, for a wide range of unsteady flows, a nearly linear pressure-drop–flow relationship, with pressure drop approximately in phase with flow.

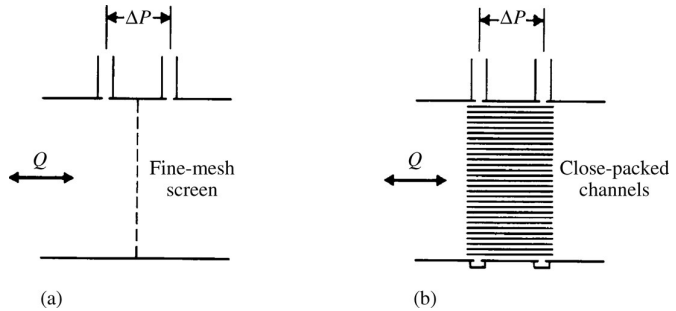

Figure 9.3 Pneumotachometer flow-resistance elements (a) screen and (b) capillary tubes or channels.

In practice, the element is mounted in a conduit of circular cross section. The pressure drop is measured across the resistance element at the wall of the conduit (within the boundary layer of the flow). The pressure tap on each side of the resistance is either a single hole through the conduit wall or multiple holes from a circumferential channel within the wall, which is connected to a common external tap.

Because the pressure drop is measured at a single radial distance from the center of the conduit, it is assumed that this pressure drop is representative of the pressure drop governing the total flow through the entire conduit cross section. Thus these flowmeters rely on the flow-resistive element to establish a consistent—though not uniform—velocity profile on each side of the element in the neighborhood of the pressure measurement. This, however, cannot be achieved independent of the ductwork in which the pneumotachometer is placed (Kreit and Sciurba, 1996). Therefore, the placement of the pressure ports and the configuration of the tubing that leads from the subject to the pneumotachometer and from the pneumotachometer to the remainder of the system are critical in determining the pressure-drop–flow relationship. This is especially important when alternating and/or high-frequency flow patterns are involved.

A number of trade-offs exist in the design and use of these sensors. The ΔP–Q relationship may be more linear for steady flow when there is a large axial separation between pressure ports than when there is a smaller separation. But during unsteady flow with high-frequency content, the pressure drop for a larger separation may be more influenced by inertial forces. If the sensor is to avoid excessive formation of vortices at high flow rates, the cross-sectional area of the conduit at the flow-resistance element must be large enough to reduce the velocity through the element. This area may be several times that of the mouth of the subject from which the gas originates, requiring an adapter or diffuser between the mouthpiece and the resistance element. If flow separation and turbulence are to be avoided as the cross-sectional area changes, the adapter should have a shallow internal angle, θ, [Figure 9.4(a)] not exceeding 15°. The shallower the angle, however, the greater is the distance between the mouth and the flow-resistance element. Symmetric drops in pressure for the same flow rate in either direction require that the geometries of the conduit on both sides of the resistance element be matched. The volume within the adapters and conduit represents a dead space for cyclic breathing. The designer, when designing the sensor, must balance the effects of decreased angle of the diffuser against the tolerable volume of dead space.

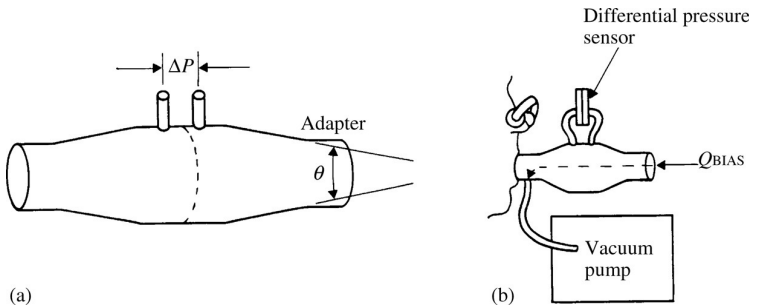

Figure 9.4 Pneumotachometer for measurements at the mouth (a) Diameter adapter that acts as a diffuser. (b) An application in which a constant flow is used to clear the dead space.

A bias flow can be used to clear this dead space. Air is drawn through the pneumotachometer from a side hole [Figure 9.4(b)] through a long tube connected to a vacuum pump. This causes a constant bias pressure drop across the pneumotachometer if the bias flow created is constant during the breathing of the patient. This approach can work well when high-frequency breathing patterns are of interest. But for low frequencies, such as those of tidal breathing, a regulating device may be required to prevent variation of the bias flow as the patient breathes.

The usable frequency range for capillary pneumotachometers is typically smaller than that for the screen type. Depending on its design, the screen-type pneumotachometer can exhibit a constant-amplitude ratio of pressure difference to flow, and zero phase shift up to as high as 70 Hz (Peslin *et al.,* 1972).

In air, the amplitude ratio of the Fleisch (capillary bundle) pneumotachometer is nearly constant at its steady-flow value up to approximately 10 Hz, increasing by 5% at 20 Hz. The phase angle between ΔP and Q increases linearly with frequency to approximately 8.5° at 10 Hz, which corresponds to an approximate 2 ms time delay between flow and pressure difference. These values change with the kinematic viscosity of the gas (Finucane *et al.,* 1972). Peslin *et al.* (1972) modeled the Fleisch pneumotachometer for frequencies up to 70 Hz by an equation of the form

$$\Delta P = RQ + L\dot{Q} \tag{9.13}$$

where L is the inertance (related to mass) of the gas in one capillary tube, defined by (7.4) and R is the flow resistance for each capillary tube, defined by (7.2). Equation (9.13) can be used as a computational algorithm to compensate the Fleisch pneumotachometer for precise measurements of a gas of constant composition at constant temperature.

EXAMPLE 9.2 A Fleisch pneumotachometer has 100 capillary tubes, each with a diameter of 1 mm and a length of 5 cm. What pressure drop occurs for a flow of 1 liter/s?

ANSWER A flow of 1 liter/s through 100 tubes is 0.00001 m^3/s through one tube. In SI units, using (7.1) and (7.2),

$$\Delta P = RF = \frac{8\eta LF}{\pi r^4} = \frac{8(0.000018)(0.05)(0.00001)}{\pi(0.0005)^4} = 367\,\text{Pa} = 3.74\,\text{cm}\,H_2O$$

An appropriately designed screen pneumotachometer may not require compensation provided by (9.13). However, it may instead be subject to equipment-generated, high-frequency noise in clinical applications. An additional point should be stressed: the frequency response of a pneumotachometer is no better than that of its associated differential pressure measurement system. It is essential that the pneumatic (acoustic) impedances, including those of the tubes and connectors between the pressure sensor and the pneumotachometer, on each side of the differential pressure sensor be balanced. This is most easily achieved by ensuring that the geometries and dimensions of the pneumatic pathways from the pneumotachometer to each side of the pressure sensor diaphragm are identical.

Equation (7.2) indicates that the resistance of the Fleisch pneumotachometer is proportional to the viscosity of the flowing gas mixture. The resistance of a screen pneumotachometer, though not computable from (7.2), is also proportional to the viscosity of the gas. The viscosity of a gas mixture depends on its composition and temperature (Turney and Blumenfeld, 1973). When inertance effects are negligible,

$$Q = \frac{\Delta P}{R(T, [F\mathrm{x}])} \tag{9.14}$$

where Q is the flow measured by the pneumotachometer for a gas mixture with species molar fractions $[F\mathrm{x}] = [N_1/N, N_2/N, \ldots, N\mathrm{x}/N]$ at absolute temperature T. Pneumotachometers are routinely calibrated for steady flow with a single calibration factor being used during experiments. Instantaneous values of T and $[F\mathrm{x}]$ are not constant during a single expiration, and their mean values change from expiration to inspiration. In particular, changes in viscosity of 10% to 15% occur from the beginning to the end of an experiment in which N_2 is washed out of the lungs by pure O_2. A continuous correction in calibration should be made when accurate results are desired.

The prevention of water-vapor condensation in a pneumotachometer is of particular importance. The capillary tubes and screen pores are easily blocked by liquid water, which decreases the effective cross-sectional area of the flow element and causes a change in resistance. Also, as water condenses, the composition of the gas mixture changes. To circumvent these problems, a common practice is to heat the pneumotachometer element, especially when more than a few consecutive breaths are to be studied. The Fleisch pneumotachometer is usually provided with an electrical resistance heater; the screen of the screen pneumotachometer can be heated by passing a current through it. In addition, heated wires can be placed inside, or heating tape or other electrical heat source can be wrapped around any conduit that carries expired gas.

9.4 LUNG VOLUME

The most commonly used indices of the mechanical status of the ventilatory system are the absolute volume and changes of volume of the gas space in the lungs achieved during various breathing maneuvers. Observe Figure 9.5 and assume that a subject's airway opening and body surface are exposed to atmospheric pressure. Then the largest volume to which the subject's lungs can be voluntarily expanded is defined as the *total lung capacity* (TLC). The smallest volume to which the subject can slowly deflate his or her lungs is the *residual volume* (RV). The volume of the lungs at the end of a quiet expiration when the respiratory muscles are relaxed is the *functional residual capacity* (FRC). The difference between TLC and RV is the *vital capacity* (VC), which defines the maximal change in volume the lungs can undergo

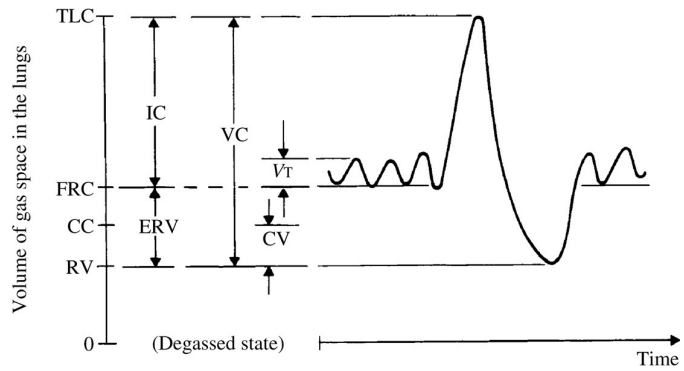

Figure 9.5 Volume ranges of the intact ventilatory system (with no external loads applied). Total lung capacity, FRC, and RV are measured as absolute volumes. Vital capacity, IC, ERV, and V_T are volume changes. Closing volume (CV) and closing capacity (CC) are obtained from a single-breath washout experiment.

during voluntary maneuvers. The vital capacity can be divided into the *inspiratory capacity* (IC = TLC – FRC) and the *expiratory reserve volume* (ERV = FRC – RV). The peak-to-peak volume change during a quiet breath is the *tidal volume* (V_T) (Petrini, 1988).

CHANGES IN LUNG VOLUME: SPIROMETRY

The measurement of changes in lung volume has been approached in two ways. One is to measure the changes in the volume of the gas space within the body during breathing by using plethysmographic techniques (discussed in Section 9.5). The second approach, referred to as *spirometry,* involves measurements of the gas passing through the airway opening. The latter measurements can provide accurate, continuous estimates of changes in lung volume only when compression of the gas in the lungs is sufficiently small. The flow of moles of gas at the airway opening can be expressed as

$$\dot{N}_{AWO} = \rho_{AWO} Q_{AWO} \cong \rho_L \dot{V}_L \tag{9.15}$$

if we neglect the net rate of diffusion into the pulmonary capillary blood. This equation can be rearranged and, if the densities are essentially constant, integrated from some initial time t_0, as follows:

$$\frac{\rho_{AWO}}{\rho_L} \int_{t_0}^{t} Q_{AWO}\, dt \cong \int_{t_0}^{t} \dot{V}_L\, dt = V_L(t) - V_L(t_0) = v_L \tag{9.16}$$

in which v_L is, according to the convention used here, the change in the volume of the lungs relative to the reference volume $V_L(t_0)$. The density ratio accounts for differences in mean temperature, pressure, and composition that may exist between the gas mixture inside the lungs and that in the measurement sensor external to the body.

For purposes of testing pulmonary function, (9.16) is frequently implemented directly by electronically integrating the output of a flowmeter placed at a subject's mouth (with the nose blocked). However, the most common procedure for estimating v_L—in use since the nineteenth century—is to continuously collect the gas passing through the airway opening and to compute the volume it occupied within the lungs. This represents a physical integration of the flow at the mouth; it is performed by a device called a *spirometer.* The widespread and historical use of this device has given rise to use of the term *spirometry* to mean the measurement of changes in lung volume for testing of pulmonary function, regardless of whether a spirometer, flowmeter plus integrator, or plethysmographic technique is used. Consequently, performance recommendations have been published by the American Thoracic Society (Anonymous, 1995a) for spirometry systems in general, regardless of the primary variable measured (volume change or flow) or the type of sensor used. The recommendations address volume range and accuracy, flow range, time interval for which data are to be collected, respiratory load imposed on the subject, and calibration standards to be met by such systems for various pulmonary function tests.

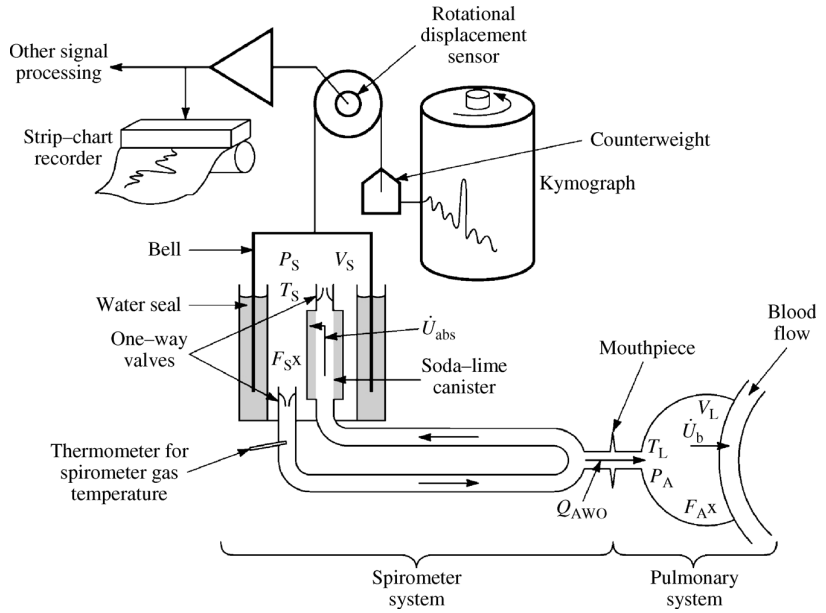

Figure 9.6 A water-sealed spirometer set up to measure slow lung-volume changes. The soda-lime and one-way-valve arrangement prevent buildup of CO_2 during rebreathing.

A spirometer is basically an expandable compartment consisting of a movable, statically counterbalanced, rigid chamber or "bell," a stationary base, and a dynamic seal between them (Figure 9.6). The seal is often water, but dry seals of various types have been used. Changes in internal volume of the spirometer, V_S, are proportional to the displacement of the bell. This motion is traditionally recorded on a rotating drum (kymograph) through direct mechanical linkage, but any displacement sensor can be used. A simple approach is to attach a single-turn, precision linear potentiometer to the shaft of the counterweight pulley and use it as a voltage divider. The electric output can then be processed or displayed.

The mouthpiece of the spirometer (Figure 9.6) is placed in the mouth of the subject, whose nose is blocked. As gas moves into and out of the spirometer, the pressure P_S of the gas in the spirometer changes, causing the bell to move. Analysis of the dynamic mechanics of a spirometer indicates that these variations in pressure are reduced by minimizing (1) the mass of the bell and counterweight and the moment of inertia of the pulley, (2) the gas space in the spirometer and tubing, (3) the surface area of the liquid seal exposed to P_S, (4) the viscous and frictional losses by appropriate choice of lubricants and type of dynamic seal, and (5) the flow resistances of any inlet and

outlet tubing and valves. During resting breathing, the pressure changes in the gas within the spirometer can be considered negligible. Therefore, only the temperature, average ambient pressure, and change in volume are needed to estimate the amount of gas exchanged with the spirometer. To use the spirometer for estimates of change in lung volume during breathing patterns of higher frequency ($>1\,\text{Hz}$) requires, in addition to the variables just mentioned, knowledge of the acoustic compliance of the gas in the spirometer (see Problem 9.3) and continuous measurement of the change of the spirometer pressure relative to ambient pressure.